



Universidad de Oviedo
Universidá d'Oviéu
University of Oviedo

Immunochematographic test for screening of surface extracellular vesicle biomarkers in plasma of patients with colorectal cancer



Gabriel Pino Peco

2021 – 2022

JULY



Prof. María Carmen Blanco López, Full Professor of Department of Physical and Analytical Chemistry in Oviedo University.

PhD Esther Serrano Pertierra, postdoctoral researcher at the Department of Physical and Analytical Chemistry in Oviedo University.

The research work entitled “Immunochromatographic test for screening of surface extracellular vesicle biomarkers in plasma of patients with colorectal cancer” has been made under our supervision by Gabriel Pino Peco, during his studies at the Master of Biotechnology of Environment and Health by Oviedo University. The work was carried out in the laboratory of the Nanoparticles, Membranes and Bioanalysis Research Group (NanoBioMem-Lablink) at the Physical and Analytical Chemistry Department in Oviedo University.

We hereby state that we have read and corrected the present Master Thesis document, and that it is suitable for its public defence by the student at the designed tribunal. Therefore, we authorize the submission of this Master Thesis to the University of Oviedo, MBEH academic commission.

In Oviedo, 14th July, 2022

Signed:

Signed:

María Carmen Blanco López

Esther Serrano Pertierra

Abstract

Colorectal cancer is one of the most frequent malignant neoplasms in the world, as well as one of the leading causes of cancer death. Affecting mostly developed countries, this cancer can be treated with a high success chance if it is detected at an early stage. However, current diagnosis methods are either non-specific or invasive and uncomfortable for patients. Thus, they are not the most suitable strategies for extensive screening of the population. Our team has been working on a detection method offering a fast, easy-to-use and non-invasive diagnosis, in the form of a lateral flow immunoassay for the measurement of surface markers in extracellular vesicles. Previously considered as cellular waste products, extracellular vesicles are now known to be involved in cell-to-cell communication, inflammation and immune response regulation. Research has also proven that extracellular vesicle composition and release are altered in tumor cells, which makes them potential biomarkers for cancer diagnosis. The present work focused on the analysis of plasma-derived extracellular vesicles containing membrane proteins CD9, CD147 and EpCAM, from samples of patients at different stages: control, low-grade adenoma, high-grade adenoma and colorectal cancer. Our aim is to understand the potential of our lateral flow immunoassay as a point-of-care device using the extracellular vesicle markers CD9, CD147 and EpCAM for the diagnosis of colorectal cancer at different clinical stages.

Resumen

El cáncer colorrectal es uno de los neoplasmas malignos más frecuentes globalmente, así como una de las principales causas de muerte por cáncer. Afectando principalmente a países desarrollados, este cáncer puede ser tratado con una alta probabilidad de éxito si detecta en un estadio temprano. Sin embargo, los métodos de diagnóstico actuales son poco específicos o incómodos e invasivos para los pacientes. Por ello no son particularmente aptos para ser utilizados en un cribado extensivo de la población. Nuestro equipo ha desarrollado un método de detección que ofrece un diagnóstico rápido, simple y no invasivo, en forma de un inmunoensayo de flujo lateral para la medida de marcadores de superficie en vesículas extracelulares. Anteriormente consideradas como productos de deshecho celular, hoy se sabe que las vesículas extracelulares participan en la comunicación intercelular, la inflamación y la regulación del sistema inmune. También se sabe que la composición y la formación de vesículas extracelulares se ve alterada en células tumorales, lo que las convierte en biomarcadores potenciales para el diagnóstico de cáncer. Éste trabajo se centra en el análisis de vesículas extracelulares plasmáticas con las proteínas de membrana CD9, CD147 y EpCAM, de muestras de pacientes en distintos estadios: control, adenoma de bajo riesgo, adenoma de alto riesgo y cáncer colorrectal. Nuestro objetivo es estudiar el potencial de nuestro inmunoensayo de flujo lateral como un dispositivo en el punto de atención, usando los marcadores de vesículas extracelulares CD9, CD147 y EpCAM para el diagnóstico de cáncer colorrectal en distintos estadios clínicos.

Abbreviations

CRC: Colorectal cancer

AdH: High-grade adenoma

AdL: Low-grade adenoma

CT: Control

EV: Extracellular vesicle

MVB: Multivesicular bodies

ILV: Intraluminal vesicle

HIV: Human immunodeficiency virus

AD: Alzheimer's disease

LFA: Lateral flow assay

LFIA: Lateral flow immunoassay

AuNP: Gold nanoparticle

PoC: Point-of-Care

FOBT: Faecal occult blood test

HsgFOBT: High-sensitivity guaiac-based FOBT

FIT: Faecal immunochemical test

CCE: Colon capsule endoscopy

SEC: Size exclusion chromatography

DLS: Dynamic light scattering

NTA: Nanoparticle tracking analysis

Index

1.	Introduction	5
1.1.	Colorectal cancer.....	5
1.1.1.	CRC, a global disease.....	5
1.1.2.	Diagnosis.....	6
1.2.	Extracellular vesicles.....	7
1.2.1.	Exosomes.....	8
1.2.2.	Microvesicles.....	10
1.2.3.	Apoptotic bodies.....	11
1.3.	Extracellular vesicles as biomarkers.....	11
1.3.1.	Potential of EVs as biomarkers.....	11
1.3.2.	Extracellular vesicles and colorectal cancer.....	14
1.4.	Isolation of extracellular vesicles.....	15
1.4.1.	Ultracentrifugation.....	15
1.4.2.	Size-based separation techniques.....	15
1.4.3.	Immunocapture.....	16
1.4.4.	Precipitation.....	16
1.5.	Detection of EVs using PoC devices.....	17
1.5.1.	PoC devices.....	17
1.5.2.	Lateral flow immunoassay.....	17
2.	Objectives.....	19
3.	Materials and methods.....	20
3.1.	Cohort of study and sample collection.....	20
3.2.	Purification of extracellular vesicles.....	20
3.3.	Conjugation of gold nanoparticles with antibodies.....	21
3.4.	Preparation of test strips.....	22
3.5.	Lateral flow assay procedure.....	23
3.6.	BCA protein quantification assay.....	23
3.7.	Size measurements by DLS.....	24
3.8.	Statistical analysis.....	25
3.8.1.	Removal of outliers.....	25
3.8.2.	Data treatment.....	25
4.	Results.....	26
4.1.	Characterization of extracellular vesicles.....	26
4.1.1.	Size distribution.....	26

4.1.2.	Total protein content.....	27
4.2.	Analysis of surface EV biomarkers.....	29
4.2.1.	Analysis of CD9 ⁺ EV by lateral flow immunoassay.....	29
4.2.2.	CD147 and EpCAM markers in CRC diagnosis.....	30
4.3.	Pilot study: effect of freezing-thawing EV fractions.....	33
5.	Discussion.....	35
6.	Conclusions.....	38
7.	Bibliography.....	39

1. Introduction

1.1. Colorectal cancer

1.1.1. CRC, a global disease

Colorectal cancer (CRC) is the third most common malignant neoplasm worldwide, with an estimated 1.9 million cases in 2020. In Spain, it is only surpassed by breast cancer in women and prostate cancer in men (Sawicki *et al.*, 2021, Spain, Globocan 2020 (<https://gco.iarc.fr/today/data/factsheets/populations/724-spain-fact-sheets.pdf>)). 40,441 new cases of CRC were detected in Spain in 2020, 24,610 in men and 15,831 in women, only behind 34,088 cases of breast cancer in women and 34,613 cases of prostate cancer in men. CRC is the second leading cause of cancer death after lung cancer, with an estimated number of 16,331 deaths in Spain in 2020.

Survival rate of patients of CRC depends on multiple factors, but is heavily influenced by the clinical stage of the cancer. In a study in southern Spain with 4,759 patients (Nuñez *et al.*, 2020), it was determined that the average five-year survival rate of CRC patients was of 55% in men and 57% in women, and that the stage of diagnosis heavily influenced this rate. In fact, patients diagnosed at an early stage showed higher five-year survival estimates than those diagnosed at later stages. The survival rates decreased from 81-89% at stage I CRC (the most localized stage) to 61-64% in phase III and only 11-12% in phase IV. This trend reveals the importance of an early diagnosis in order to maximize the survival rate of CRC patients.

As reviewed by (Sawicki *et al.*, 2021), multiple risk factors increase the chance of developing colorectal cancer. Certain genetic and family factors increase the risk of CRC, such as a family history involving cancer, diabetes mellitus, cholecystectomy, inflammatory bowel disease or colon polyps. Studies reveal that people with first degree relatives affected by cancer have twice the risk of developing CRC than someone with no family history. In some cases, hereditary syndromes are responsible for CRC (estimated at 2 to 8% of cases). Patients with Lynch syndrome, an autosomal disease involving a mutation in mismatch repair genes, present a chance of CRC of 20% by the age of 50 and of 80% by the age of 80. Familial adenomatous polyposis is another autosomal disease affecting the tumor suppressing APC gene, and if untreated the patients develop CRC at a relatively young age.

The lifestyle of a person may also contribute to an increased risk of CRC (Sawicki *et al.*, 2021), such as the consumption of red meat and processed meat (salted, smoked,

spiced, cured ...). On the other hand, consumption of vegetal fibers, calcium and vitamin D may reduce the risk. Diet influences the composition of the gut microbial community, which also constitutes a factor influencing CRC. Sedentary lifestyles, overweight, obesity, alcohol consumption and tobacco are risk factors related to CRC as well. Countries with a high development index present an overall higher CRC incidence (Figure 1) which may be related to all these risk factors together with an increasing lifespan of the population.

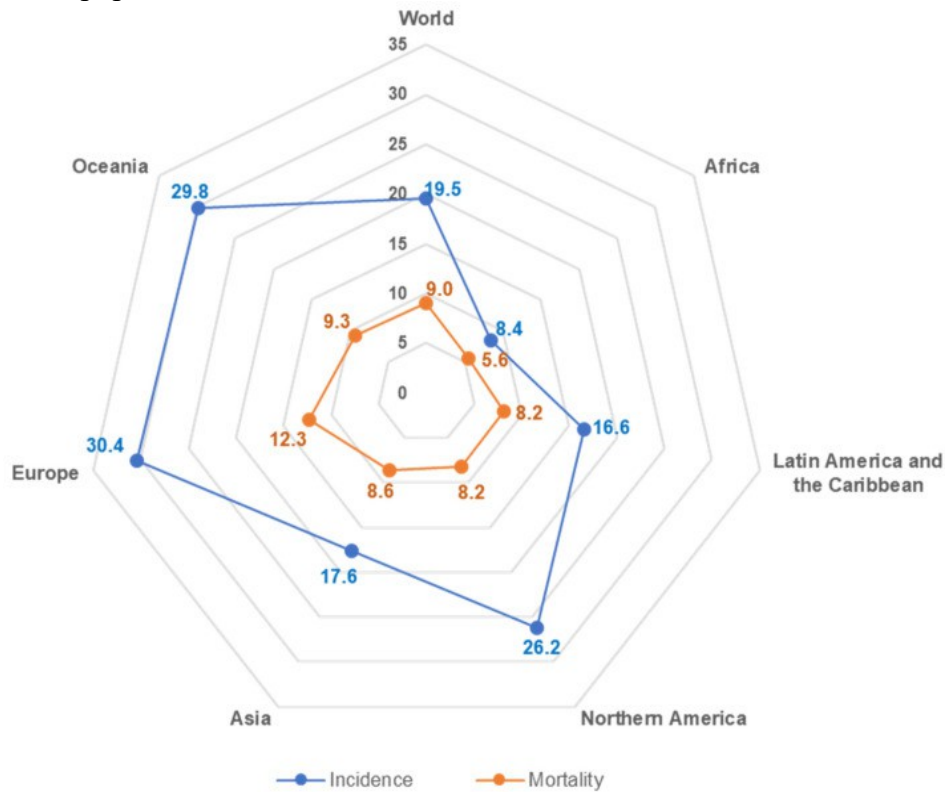


Figure 1: Standardized incidence and mortality rates for CRC for both sexes in 2020, per 100,000. (Sawicki *et al.*, 2021)

1.1.2. Diagnosis

Due to the importance of an early diagnosis for CRC treatment, the implementation of screening programs have been carried out in some countries. Those programs are based on different techniques that are currently in use to detect this cancer.

The faecal occult blood test (FOBT) is the most widely used screening method for CRC detection, and it measures the presence of blood in faeces samples, caused by the bleeding of the carcinoma. Two formats of these FOBT are available: the guaiac-based test (HsgFOBT) and the immunochemical assay (FIT). FIT specifically targets human haemoglobin, and is less restrictive with the patient's diet during the preparation for testing than HsgFOBT (meat consumption can interfere with this last test) (Sawicki *et*

al., 2021). However, faecal occult blood based methods present sensitivity issues. False negatives are common for early stages and for some cancers that do not bleed. Moreover, false positives are highly present due to non-specific bleeding or meat consumption (Strul and Arber, 2002). Therefore, while faecal occult blood tests are useful for extensive screening, they require further testing using a different method.

Endoscopic screening is the most reliable method for CRC detection, and involves a direct, though invasive, observation of the rectum and the entire colon. Colonoscopy presents a high sensibility and specificity for CRC detection, and biopsies may be taken during the procedure. However, this method presents some disadvantages and risks. It is an expensive method requiring the participation of specialist health professionals. The preparation of the colonoscopy starts some days before and it involves the use of laxatives and strict diet to clean the bowels, and the patient could experience discomfort after the procedure. Moreover, there is a small risk of complications such as bleeding, infections and bowel damage or perforations (Sawicki *et al.*, 2021, Colonoscopy Risks, WebMD (<https://www.webmd.com/colorectal-cancer/colonoscopy-risks>)).

Colon Capsule Endoscopy (CCE) is a non-invasive, alternative method to colonoscopy, recommended in cases of moderate CRC risk and when colonoscopy is not recommended. It involves the use of an ingestible capsule containing cameras to detect CRC (Sawicki *et al.*, 2021, Han *et al.*, 2016). Similarly to the latter, it requires a prior preparation with laxatives, and unlike this one, it is non invasive, reducing its risks. However, biopsies cannot be collected with this technique.

Other non-invasive imaging techniques exist, but their effectiveness is limited, due to the difficulty to detect small polyps in the soft bowel tissues (Sawicki *et al.*, 2021).

Due to the limitations of the current detection methods, there is a need for rapid and non-invasive detection methods for CRC diagnosis. For this purpose, new biomarkers and techniques are sought, and among them, extracellular vesicles are strong candidates for this role.

1.2. Extracellular vesicles

Extracellular vesicles (EVs) are membranous structures present in biological fluids and released by cells. This term is actually used to describe a broad and heterogeneous

group of elements with different structures, composition and origin. The variety of EVs offers high potential as new generation biomarkers for prognostics and diagnosis of a variety of diseases. Among EVs, two major groups can be distinguished: exosomes and microvesicles (Van Niel *et al.*, 2018).

1.2.1. Exosomes

Exosomes are extracellular vesicles with an estimated size of 30 to 150 nm. They were identified in biological fluids in the late 1980s, when they were thought to be cellular waste products formed as a result of cell damage, or during cellular metabolism and homeostasis. By the mid 1990s, they were reported to be secreted by B lymphocytes and dendritic cells, and were thought to be involved in the regulation of immune responses. Currently, exosomes are a prolific subject of study. They carry a complex cargo (Figure 2), which depends on the cell of origin and its physiological state, and deliver it to recipient cells, thus participating in the intercellular communication in many processes. Such processes include antigen presentation, immune response, and signal transduction (Van Niel *et al.*, 2018, Doyle and Wang, 2019, Zhang Y. *et al.*,

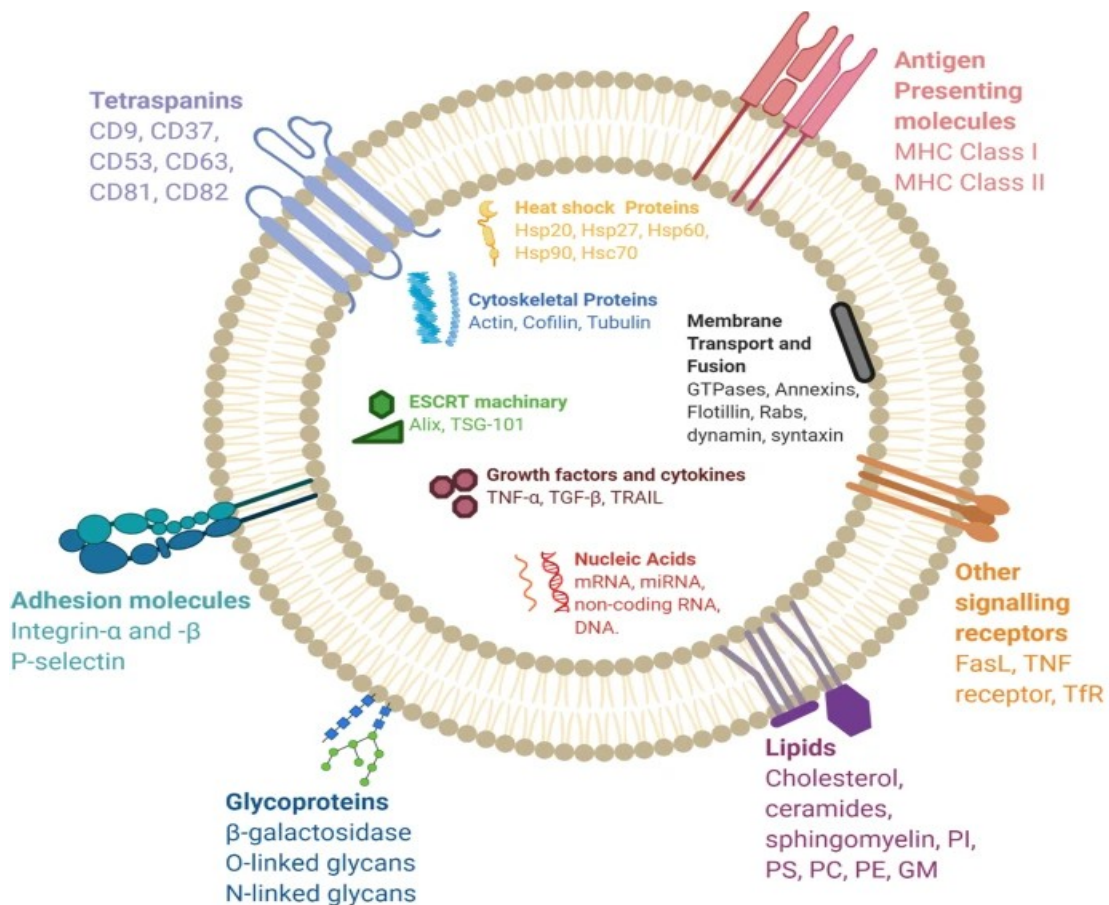


Figure 2: composition of exosomes. Source: (Gurung *et al.*, 2021)

2019). Exosomes are enriched in proteins, and carry a variety of them such as tetraspanins (*e.g.* CD9, CD63, CD81), heat shock proteins, cell adhesion proteins, antigen presentation proteins, signalling proteins, membrane transport proteins, exosome release related proteins, enzymes, etc. In addition, RNA sequences, mostly microRNA (miRNA) and ribosomal RNA, which may be involved in intercellular communications, are also found in exosomes. Among those, RNA sequences involved in angiogenesis, exocytosis, haematopoiesis as well as tumor cell growth and adhesion modulation are known to be present in these structures. Exosomes are also enriched in lipids such as cholesterol, arachidonic acid, phosphatidylserine, etc. They are also thought to be responsible of cell-to-cell communication via signalling pathways triggering lipid dependent responses in the recipient cells (Zhang Y. *et al.*, 2019).

Unlike microvesicles, exosomes are not directly formed by budding of the cellular membrane. Instead, they are formed via the invagination of the endosomal membrane of limited multivesicular bodies (MVB), as can be seen in Figure 3. The intraluminal vesicles (ILVs) formed inside the MVBs, when released into the extracellular environment, are called exosomes. The endosomal sorting complex required for endosome transport (ESCRT) is one of the main pathways of exosome formation, although MVB and ILV may be formed by ESCRT-independent pathways

In this process, tetraspanins play a role in protein anchoring to the membrane, leading to cargo sorting in ILVs. Tetraspanins also seem to play a role in the fate of MVBs, being

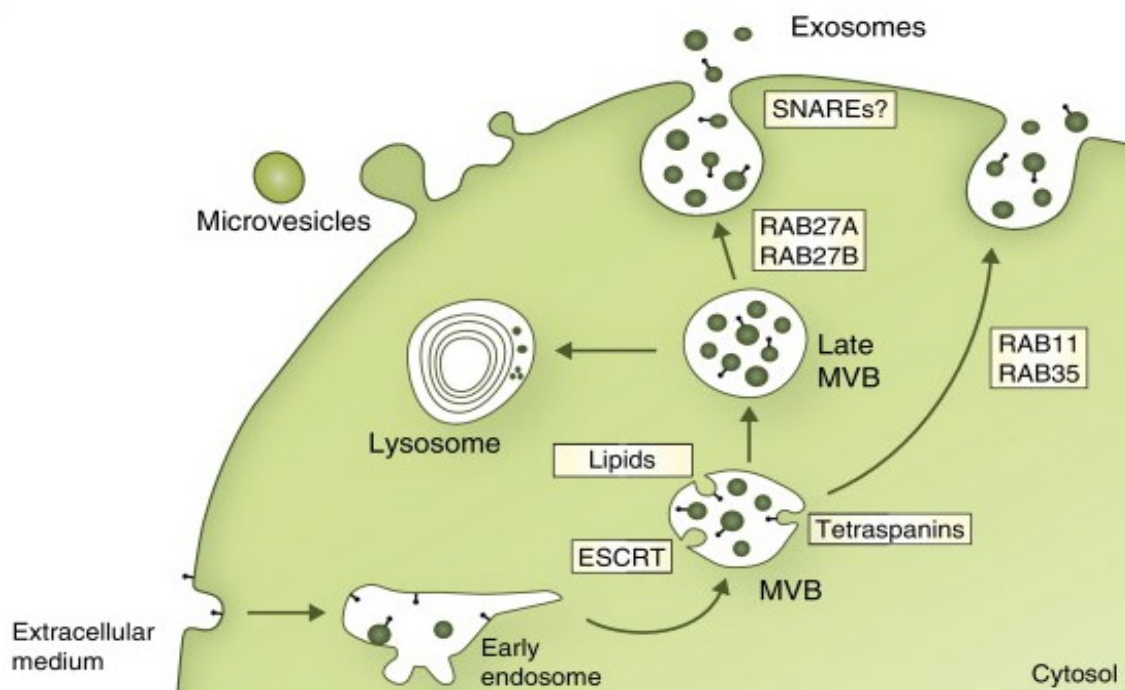


Figure 3: Biogenesis and secretion of exosomes. Source: (Kowal *et al.*, 2014)

degradation by a lysosome or fusion with the membrane and release of exosomes (see figure 3) (Gurung *et al.*, 2021). In this respect, cholesterol content has also been linked to the final destination of MVBs (Doyle and Wang, 2019).

Finally, the Rab GTPase family has been identified as a fundamental actor in MVB trafficking inside the cell. The interaction of these Rab GTPases and SNARE proteins in the cell membrane is thought to induce exosome release (Gurung *et al.*, 2021).

1.2.2. Microvesicles

As previously mentioned, microvesicles shed directly from the cell membrane and can reach sizes in the range of the micrometric scale, since they are not limited by the size of MVBs. Microvesicles are released by many cell types in normal and/or altered physiological states. For this reason, microvesicles are a highly heterogeneous group (similar to exosomes) containing a wide variety of cargoes (proteins, RNA, lipids) with different functions, as seen in figure 4 (Tricarico *et al.*, 2017).

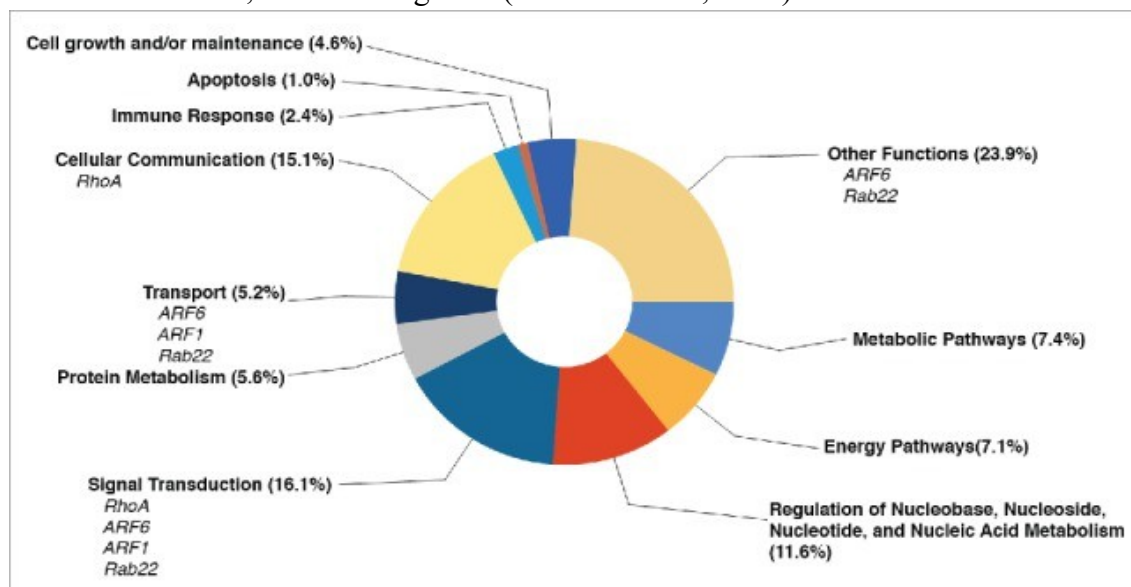


Figure 4: Common biological functions of microvesicle protein cargo identified in Vesiclepedia database. Source: (Tricarico *et al.*, 2017)

Through cell-to-cell communication, microvesicles are known to perform various physiological roles. Several works have revealed their importance in the circulatory system during coagulation. In particular, platelet derived microvesicles have been reported to have up to 100-fold greater coagulant activity than platelets themselves. They are also known to have functional roles in the immune response, aiding to combat infections and regulating inflammation. Tumor cells can release a large number of microvesicles, which can contribute to the spread and development of the disease. For

instance, tumor-derived microvesicles may play a role in the transfer of growth factors, angiogenesis, development of drug resistance, evasion and suppression of the immune system, and facilitation of cell mobility and tumor invasion. Microvesicles also play a role in communication between stem cells and tissue cells, leading to the mediation of functions such as tissue repair, cell proliferation, apoptosis, or angiogenesis ... (Tricarico *et al.*, 2017, Muralidharan-Chari *et al.*, 2010).

Microvesicle biogenesis is fundamentally different to that of exosomes, although they share some common actors. Cargo trafficking happens via selective recruitment of proteins and RNA. ARF6 and Rab22a may play an important function in protein trafficking. v-SNAREs also take part in cargo trafficking and convergence into the shedding microvesicles. RNA cargo requires RNA trafficking proteins for its transport, such as CSE1L or T-cell internal antigen 1 (Tricarico *et al.*, 2017).

For microvesicle shedding, processes such as the interaction of proteins ARRDC1 and TSG101, lateral pressure in the membrane due to interactions in a crowded protein environment, or an alteration and reorganization in membrane lipids may be involved in membrane curvature before shedding. The actual vesicle shedding, requires the contractile machinery formed by the interaction of actin and myosin, regulated by proteins such as ARF1 and ARF6, that trigger a phosphorylation of myosin through the activation of kinases (Tricarico *et al.*, 2017).

1.2.3. Apoptotic bodies

With sizes of up to 5 μm , apoptotic bodies are another type of EV. Unlike exosomes and microvesicles, they are not released through a regulated method from functional cells. These vesicles contain information of dying cells, such as organelles and DNA, and their composition is rather similar to a cell lysate (Doyle and Wang, 2019).

1.3. Extracellular vesicles as biomarkers

1.3.1. Potential of EVs as biomarkers

Due to their presence in biological fluids and their varied cargo content, EVs are good candidates as non-invasive biomarkers and therapeutic agents. Composition and abundance of EVs depends on the cell of origin, as well as its on physiological state. The process of EV biogenesis depends on a number of elements, participating in cargo trafficking and vesicle shedding. Since those elements are highly regulated within the

cell, a modification of the physiological state of the cells will lead to a difference in vesicle cargo and release rate. Therefore, cells in an altered state, such as cancer cells, deliver a different EV profile than normal cells. Through the identification of the adequate markers, rapid and efficient diagnosis can be achieved in a non-invasive format (Doyle and Wang, 2019, Zhang Y. *et al.*, 2019, Tricarico *et al.*, 2017, Zhang Y. *et al.*, 2021), allowing new early screening systems for a number of pathologies. Exosomes and microvesicles are also candidates for therapeutic treatments as vaccines due to their antigen presenting capabilities, for other immunological applications, as drug delivery systems and as a therapeutic tool (Doyle and Wang, 2019, Zhang Y. *et al.*, 2021). The promise of EVs as non-invasive biomarkers and therapeutic agents has therefore led to an increase in the scientific interest for them, opening a variety of research lines in this field. Since the present work focuses on the use of EV proteins as markers, applications of EVs as diagnosis tools will be reviewed in the following paragraphs.

EVs have been found to be potential markers for HIV infection and immune response. A study revealed that in HIV-positive patients, EV concentration was statistically higher than in healthy control patients (Chettimada *et al.*, 2018). Moreover, the levels of the markers CD9, CD63 and HSP70 were significantly higher in infected patients, the first two presenting a higher count even in a normalized EV number. CD9 and CD63 were also found to correlate with oxidative stress and immune activation markers, as well as with the reduction of anti-inflammatory markers. Proteomic analyses also revealed immune activation markers CD14, CRP, HLA-A and HLA-B to be detectable only in HIV-positive patient EVs.

EVs are also of interest for the identification of neurodegenerative disease biomarkers. Alzheimer's disease (AD) is a progressive neurodegenerative disorder estimated to affect 50 million people worldwide. Amyloid beta ($A\beta$) and tau proteins are known to be present in AD patient brains, but current diagnosis and follow-up of the disease lack reliable non-invasive biomarkers. Brain-derived exosomes are known to cross the blood-brain barrier, making them potential non-invasive biomarkers, in contrast with the more invasive procedure of collecting cerebrospinal fluid. In a meta-analysis comprising of multiple previous studies, the authors identified proteins $A\beta_{42}$, t-tau, p-T181-tau, and p-S396-tau as potential brain-derived exosome markers for AD diagnosis (Kim *et al.*, 2021).

Cancer diagnosis through EV-derived markers is an increasing line of study. As

previously stated, it is known that cancer cells can use EVs to their own advantage, increasing their invasiveness and neutralizing the immune system. Tumor cells may use EVs as primary actors in the development of cancer, as their exposure to a hostile environment drives a selection of the most adapted cells, and with their complex cargo and capacity for cell-to-cell communication, EVs constitute a useful tool for tumor growth and adaptation. In the tumor microenvironment, EVs are overproduced, and in fact some experimental data revealed a correlation between tumor mass and exosomes in plasma (Logozzi *et al.*, 2020). Those same characteristics make EVs an excellent tool for cancer detection and treatment. Tumor suppression techniques could benefit from EVs as a tool for targeted drug delivery, as well as as an anti-tumoral vaccine stimulating the immune system (Dai *et al.*, 2020). Furthermore, the use of EVs by tumor cells could also become a target itself, with EV-production suppression therapies as an anti-tumoral treatment (Logozzi *et al.*, 2020).

The modification of both EV count and cargo type opens a myriad of opportunities for cancer detection and biomarkers. Protein biomarkers are good candidates for cancer detection, due to the information provided by the upregulation or downregulation of specific markers in tumor cells. Many proteins have been found to have modified expression rates in cancer derived EVs. For example, lung cancer EVs are known to contain several protein markers that can be used for its identification, such as epidermal growth factor receptor, CD151, CD171 and tetraspanin 8 (Reclusa *et al.*, 2017). Glypican 1, a protein involved in several signalling pathways, was also reported to have potential as a biomarker, since it promotes angiogenesis and metastasis in pancreatic cancer, and it is upregulated in tumor-derived exosomes (Liu H. *et al.*, 2021). Moreover, post-translational modifications of proteins, such as phosphorylation, ubiquitination, oxidation and others, can also be influenced by an alteration in their cells during oncogenesis (Shen *et al.*, 2020).

Besides the protein content, EVs contain nucleic acids and lipids that may be good candidates for biomarkers. High levels of miR-105 RNA may be indicative of tumor metastasis, and LISCH7 mRNA was overexpressed in EVs from colon cancer patients (Shen *et al.*, 2020). Studies focusing on the detection of thyroid cancer have also revealed circulating exosomal miRNAs such as miR-146b-5p and miR-222-3p, as well as circular RNAs (circRNA) circRASSF2 as potential markers (Feng *et al.*, 2020). Some RNA sequences, such as miRNA-21, are overexpressed in lung cancer patients, while its levels are non-detectable in healthy patients (Reclusa *et al.*, 2017).

1.3.2. Extracellular vesicles and colorectal cancer

The EV membrane is known to contain a variety of proteins in their surface: proteins from the ESCRT complexes, heat shock proteins, tetraspanins such as CD9, CD63 and CD81, etc. Other proteins are found more specifically in some types of exosomes, such as annexin or Rab proteins. Through proteomic analyses of the composition of EVs, it has been possible to identify the presence of certain markers in CRC patients in those vesicles (Hon *et al.*, 2017). Through a detection method using photosensitizer-beads, it was confirmed that the levels of CD147 in serum-derived EVs increased in CRC patients (Yoshioka *et al.*, 2014). A33 and epithelial cell adhesion molecule (EpCAM), known to be related with tumor progression, were revealed to be present in exosomes derived from human colon carcinoma cell line LIM1863 (Tauro *et al.*, 2013), and their overexpression was related to the progression of CRC (Liu H. *et al.*, 2021). Other surface proteins, such as CD23, are also reported to be linked to CRC, as well as to other types of malignancies (Liu H. *et al.*, 2021). However, it must also be taken into account that EV biogenesis is a highly regulated process, and involves complex cargo trafficking mechanisms. Therefore, a modification in the expression of a protein in the cancer cells does not necessarily mean that the same will be observed in EVs. This is observed in a proteomic analysis (Tauro *et al.*, 2013), where the EV content of some proteins, such as IGF1 and HSP90, did not match their reported expression in cancer cells.

Certain nucleic acids, such as miRNA, also constitute reliable markers for CRC. It is known that overexpression of miR-19a-3p, miR-223-3p, miR-92a-3p and miR-422a is linked to early cancer development (Zheng *et al.*, 2014), excess of miR-19a promotes tumor invasion, cancer cell proliferation and tumor recurrence (Hon *et al.*, 2017, Matsumura *et al.*, 2015), and miR-210 upregulation increases metastasis (Qu *et al.*, 2014). Other exosomal miRNAs have also been correlated to CRC. For example, miR-1229 has been proposed as a biomarker offering high specificity and sensibility to CRC (Hon *et al.*, 2017). Aside from miRNAs, it is also known that some mRNAs, such as Δ Np73, long-non-coding RNAs as CRNDE-h, and circRNAs such as circFAT1 are expressed differentially (either up or downregulated) in CRC-cell derived exosomes (Hon *et al.*, 2017).

1.4. Isolation of extracellular vesicles

While EVs are promising candidates for a variety of clinical diagnosis techniques, the lack of a standardized isolation method remains a major issue. Currently, isolation techniques separate/enrich EVs as a whole, regardless their biogenesis pathway. For this reason, the generic term EV is preferred when the research does not establish specific markers of subcellular origin. Currently, multiple strategies allow for isolation of EVs, each with their own advantages and deficiencies (Table 1).

Table 1: comparison of exosome isolation techniques. Based in (Chen J. *et al.*, 2022)

Technique	Purity	Yield	Time	Characteristics
Ultracentrifugation	Medium	Low	Medium to long	Complex, requires specialized equipment
Density gradient centrifugation	High	Low	Long	Complex, requires specialized equipment
Ultrafiltration	High	Low to medium	Medium	Can damage vesicles
Size Exclusion Chromatography	High	Medium	Medium to long	Used in combination with ultrafiltration or ultracentrifugation
Immunocapture	High	Medium	Medium to long	Expensive, but high specificity.
Precipitation	Low	High	Short	Cheap and simple, but extract is of low purity.

1.4.1. Ultracentrifugation

Ultracentrifugation is the gold standard for EV isolation. Differential ultracentrifugation makes use of multiple centrifugation steps in order to isolate EVs from the rest of components of the extracellular matrix and pellet them, making use of their density, size and shape. On the other hand, density gradient centrifugation is based on a centrifugation stage in a gradient solution, allowing to separate various compounds based on their densities. Those methods allow to obtain an extract of good purity at a low cost and without extensive sample pretreatment, but is time consuming and delivers low yields, therefore requiring large volumes of sample (Doyle and Wang, 2019).

1.4.2. Size-based separation techniques

Ultrafiltration techniques allow to separate compounds based on their size. By using large pore filters, large debris and apoptotic bodies can be removed from the solution,

and small pore filters will capture EVs while letting through smaller contaminants. This method is faster than ultracentrifugation, but the vesicles can be damaged, and clogging of filters may negatively affect the yield (Doyle and Wang, 2019).

Size exclusion chromatography (SEC) also separates EVs by their size. It is often used in combination with ultracentrifugation or ultrafiltration, as a way to purify EV fractions obtained. It prevents damage to the vesicles, but is slow, requiring run times of several hours (Doyle and Wang, 2019).

1.4.3. Immunocapture

Immunocapture assays use the interaction antigen-antibody to isolate EVs by binding a protein in their surface. ELISA based assays immobilize the target on the surface of a microplate. Then, the vesicles can be quantified or eluted. However, it limits the sample volume and presents limited yields. Magnetic immunocapture may overcome these limitations, by enabling the separation of EVs in larger volume samples. Moreover, due to the higher effective surface of nanoparticles, higher yields can be obtained. Finally, micro-fluidic assays are an alternative offering fast processing times for small sample volumes. Immunoassays offer both advantages and inconveniences. Generally, they offer higher purity but lower yields than other techniques. The specificity of antibodies allows to target specific EV types, but it is limited to vesicles with the adequate surface protein, excluding some of the EVs from the analysis. It also requires pretreatment of the sample (Doyle and Wang, 2019).

1.4.4. Precipitation

Precipitation techniques use specific compounds to precipitate EVs. Polyethylene-glycol (PEG) is a water excluding element that captures water molecules and causes EVs to precipitate. Lectins are proteins that bind carbohydrates in the surface of exosomes, causing them to lose solubility. Precipitates can be collected by centrifugation at low speed. These methods provide a fast and simple isolation with high return yields, but present low specificity, since other compounds co-precipitate with the EVs (Doyle and Wang, 2019). Due to its simplicity, precipitation methods are well suited for diagnosis in clinical settings. Therefore, the present work uses this method for the study of plasma-derived EV.

1.5. Detection of EVs using PoC devices

1.5.1. PoC devices

Point-of-care devices (PoC) were originally introduced roughly 40 years ago, and they have been in continuous development through the advances in technology. Their use has been increasing as a result of the need to decrease healthcare costs. With the current trend to individualize healthcare, many healthcare procedures have been switched from a more expensive centralised model to a PoC method where patients can obtain fast and reliable responses without moving to a healthcare center or requiring the intervention of a health professional (St John and Price, 2014).

St John and Price (2014) state that a PoC device must present four key requirements:

1. Simplicity of use.
2. Robustness of reagents and consumables in both storage and usage.
3. Concordant results with an equivalent established laboratory method.
4. Safety of usage for consumables, reagents and device.

1.5.2. Lateral flow immunoassay

Lateral flow assays (LFA) are currently in use as PoC devices due to their low cost and analysis time, as well as their simplicity. Those paper based tests rely on the generation of a signal upon binding of the analyte to a band in a paper strip. The classical LFA format comes in an immunoassay format, with antibodies bound to the analytical band, causing the binding of the analyte, and are used in a number of qualitative measurements and diagnosis, such as the pregnancy test measuring human chorionic gonadotropin or infection by SARS-CoV-2, influenza virus, *Streptococcus* or other pathogens (Liu Y. *et al.*, 2021).

LFAs, on the other hand, lack the sensitivity of other analytical methods. ELISA tests can reach sensitivities on the pM and fM scale, while PCR can reach the aM scale. However, those tests are expensive, complex and time consuming to be used as PoC devices, and therefore unsuitable for extensive screening of the population (figure 5). The use of LFA as a quantitative tool could prove to be a notable development in the PoC industry. Ways to improve both sensitivity and selectivity of LFA are sought, and several strategies are in place to achieve this goal. The first involves preconcentration or preamplification of analytes, reaching ELISA sensitivity levels, and in some cases, PCR levels. However, necessary sample preparation techniques increase assay complexity,

cost and processing time, reducing their suitability as PoC tests. Assay optimization strategies focus on the modification of the materials, the binding mechanism and running buffers, in order to optimize the kinetics of the assay and obtain improved sensitivities. Finally, signal amplification centers in increasing the response to analyte binding. It is achieved through a series of strategies, such as electrochemical detection, surface-enhanced Raman scattering, fluorescence, magnetic and photothermal strategies (Liu Y. *et al.*, 2021).

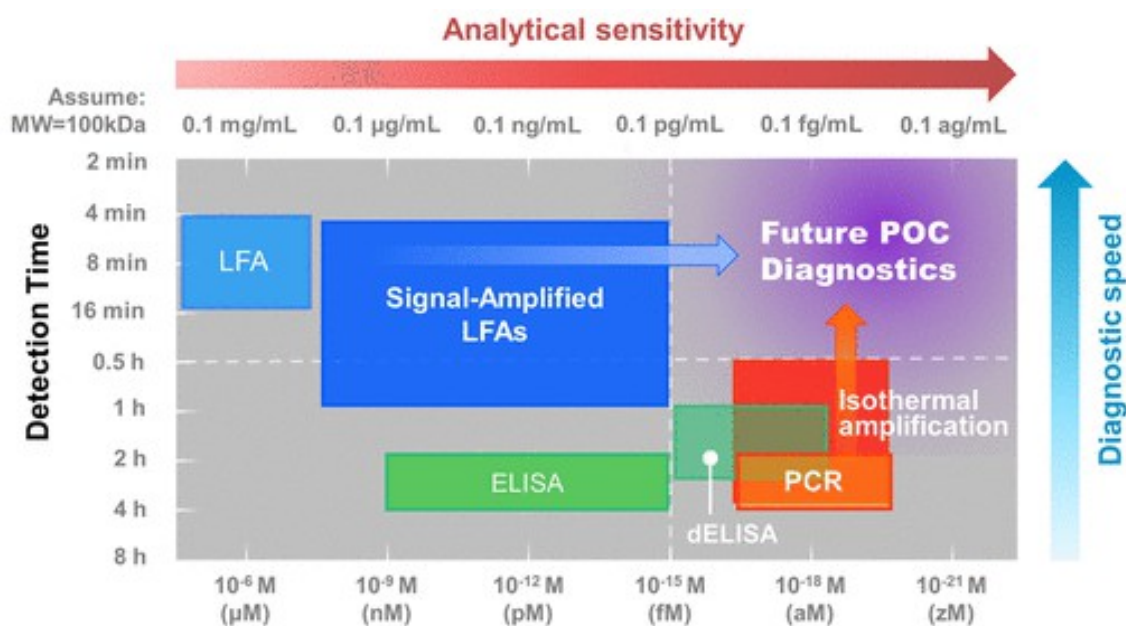


Figure 5: Comparison of analytical sensitivity and detection speed of several diagnosis tools. Source: (Liu Y. *et al.*, 2021)

Our approach focuses on the use of a lateral flow immunoassay (LFIA) using gold nanoparticles (AuNPs) to detect EVs. Antibody-bound AuNPs bind EVs and produce a colouration of the test strips. Detection through a reflective measurement is then used to quantify the EVs captured on the test line. Our research group has already worked in the application of this lateral flow assay for the diagnosis of chronic fatigue syndrome (Castro-Marrero *et al.*, 2018). This technique constitutes a potential tool as PoC device, but the identification of novel and promising biomarkers is also required.

2. Objectives

As a new source of biomarkers, EVs constitute an important and increasing field of research. They are present in numerous biological fluids, and their composition and release can be altered when the physiological state of the cell of origin is perturbed. Our approach intended to verify the performance of our LFIA in the detection of EV markers CD9, CD147 and EpCAM for the diagnosis of CRC, offering a fast, simple and non-invasive PoC device that could be of use in population screenings.

This work was carried out under the framework of the project “Nanomaterials based rapid tests for extracellular vesicles biomarkers. Applications in cancer and neurodegenerative diseases” (MCI-21-PID2020-119087RB-I00).

Our objectives were:

- Characterization of EVs in order to understand further the dynamics of EV populations in different clinical groups.
- Identification of new biomarkers for CRC by analyzing the variations in EV populations containing membrane proteins CD9, CD147 and EpCAM.
- Testing of the LFIA developed by our team, and determination of its potential as a PoC device.
- Determination of the effects caused by freezing-thawing EV fractions, to further standardize our analytical procedure.

3. Materials and methods

3.1. Cohort of study and sample collection

Patients who tested positive in a fecal occult blood test and that were about to undergo a colonoscopy were recruited at Hospital Universitario de San Agustín, after obtaining written informed consent. Details of the cohort are presented in table 2.

Patients were classified in four groups:

- Group I: patients with no pathological findings during colonoscopy (CT).
- Group II: patients with low-grade adenomas (AdL).
- Group III: patients with high-grade adenomas (AdH).
- Group IV: patients with adenocarcinomas (CRC).

Peripheral venous blood was collected in 10 mL Vacutainer (Becton Dickinson) tubes with EDTA as an anticoagulant after discarding the first milliliter and processed within 30 min of collection. Blood was first centrifuged for 30 min at 1550 g to remove cells. Aliquots of plasma were stored at -80°C until use.

Table 2: Details of the cohort.

Groups	CT	AdL	AdH	CRC	Total
Patient number	23	4	23	18	68
Male	10 (43%)	3 (75%)	19 (83%)	12 (67%)	44 (65%)
Female	13 (57%)	1 (25%)	4 (17%)	6 (33%)	24 (35%)
Age	61.6 \pm 4.3	63 \pm 6.5	61.8 \pm 5.8	67.9 \pm 11.8	63.4 \pm 7.9
Smoker	5 (22%)	0	8 (34%)	3 (17%)	16 (24%)
Alcohol	4 (17%)	1 (25%)	5 (22%)	6 (33%)	16 (24%)
Dyslipidaemia	11 (48%)	3 (75%)	10 (43%)	8 (44%)	32 (47%)
Obesity	7 (30%)	2 (50%)	10 (43%)	6 (33%)	25 (37%)

3.2. Purification of extracellular vesicles

Plasma-derived EV were isolated using a precipitation reagent (ExoQuick™, System Biosciences, Palo Alto, CA, ref: EXOQ5™-1) according to the manufacturer's instructions, as shown in figure 6. A starting volume of 110 μl of plasma samples was centrifuged for 20 min at 3200g to remove cell debris and platelets. 100 μl of supernatant were recovered. Sample was treated with 0.8 μl of thrombin (550U* ml^{-1} in PBS) in order to induce clotting of fibrin, and incubated for 5 min at room temperature.

A centrifugation of 5 min at 6800g was done. 80 μ l of supernatant were recovered, and 21 μ l ExoQuick reagent were added, followed by a homogenization of the solution by shaking. After 1h of incubation at 4°C, samples were centrifuged for 30 min at 1700g. The supernatant was then recovered as negative control (EV-depleted plasma), and the pellets were centrifuged 5 min at 1700g. The remaining supernatant was discarded, and the pellets were resuspended in 20 μ l HEPES buffer (10 mM, pH 7.4). EV fractions were then analyzed by LFIA or stored at -80°C.

3.3. Conjugation of gold nanoparticles with antibodies

Antibodies were conjugated to gold nanoparticles by passive adsorption, as seen in figure 7. The detection antibody (anti-human CD63; clone Tea3/18, Immunostep) was added into 1.5 ml of Gold Nanoparticles (AuNP), (40 nm, BBI solutions) at a concentration of 0.15 mg/mL. This addition was done progressively to prevent destabilization of AuNPs. The mixture was then incubated in a rotatory device for 1h at room temperature. After incubation, 100 μ l of Bovine Serum Albumin (BSA, Sigma-Aldrich, ref: A4503-50G) solution (1 mg/mL, in PBS buffer 10 mM, pH 7.4) was added

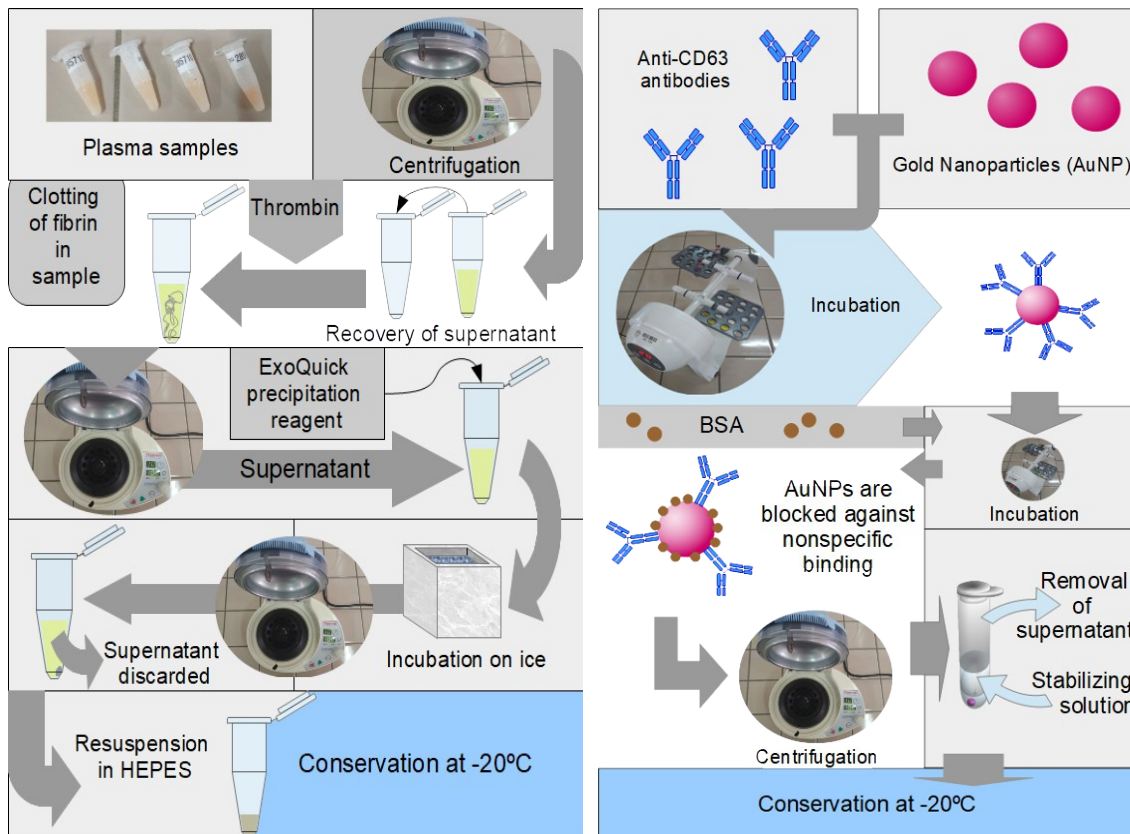


Figure 6: process of EV isolation from plasma samples.

Figure 7: conjugation of AuNPs to anti-CD63 antibodies.

progressively in order to block the remaining surface of the AuNPs and to prevent nonspecific binding. The nanoparticles were incubated for 45 minutes at room temperature. The AuNP-Ab conjugates were divided into two microcentrifuge tubes and centrifuged 20 min at 6800g. After centrifugation, 700 μ l of supernatant were discarded from each tube and the remaining pellet was cooled at 4°C for 10 - 15 min and subsequently resuspended in 100 μ l of stabilizing solution (BSA 10 μ g/mL, sucrose 100 μ g/mL, PBS 2 mM, pH 7.4). The AuNP-Ab conjugates were stored at -20°C until use.

3.4. Preparation of test strips

A nitrocellulose membrane (Millipore HI-Flow Plus, HF07504XSS) was assembled on top of a plastic backing card. Antibodies anti-CD9 (clone VJ1/20; Immunostep), anti-CD147 (clone VJ1/9; Immunostep) or anti-EpCAM (clone VU-1D9; Immunostep) were immobilized on the nitrocellulose membrane as test lines, whereas mouse anti-IgG antibody was immobilized as the control line. In all cases, the concentration of the antibodies used was 1 mg/ml, and they were dispensed at a rate of 0.100 μ l/mm, using a dispenser (Imagene Technology, IsoFlow dispenser). The porous nature of the membrane allows for the antibodies to bind to it and for the sample to flow by capillarity. Printed cards are left to dry for over 1h at 37°C. The conjugate pad (Millipore, Glass Fibre, GFCP001000), used for absorbing the test solution and allowing it to flow into the membrane, and the absorbent pad (Whatman, ref. 81162250), which stores excess solution after it has flown through the membrane, were assembled on top of the card, to either side of the membrane and slightly overlapping it. Cards were kept at room temperature in dry conditions until use. Figure 8 shows a representation of a test card.

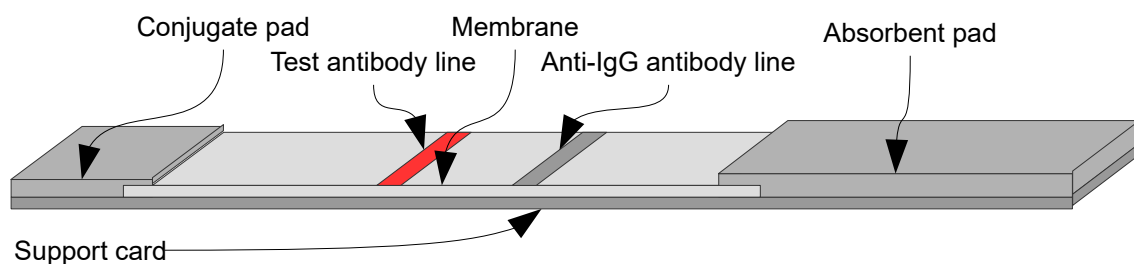


Figure 8: graphical representation of a test card. Test antibody can be either anti-CD9, anti-CD147 or anti-EpCAM.

3.5. Lateral flow assay procedure

The test cards were cut into 4 mm width strips. The LFIA tests were carried out as follows (Figure 9): 1 μ l of EV samples was mixed with 10 μ l of AuNP- α CD63. Then running buffer (BSA 10 mg/mL, tween-20 0.05%, NaCl 150 mM, HEPES buffer 10 mM, pH 7.4) was added to

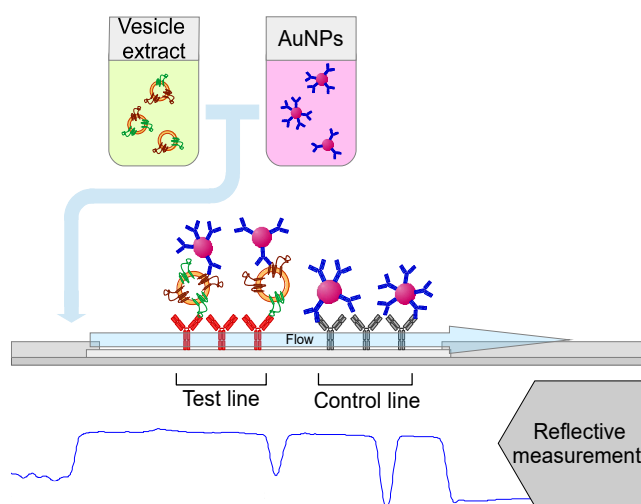


Figure 9: representation of the LFIA process used in this study.

a final volume of 100 μ L. Tests strips were then introduced into the test solution, which flows from the conjugate pad, through the nitrocellulose membrane and into the absorbent pad. Colour bands formed by the binding of the AuNPs to the antibody lines were read 15 min afterwards in an optical reader (QIAGEN, ESEQuant LR3) to quantify their intensity.

3.6. BCA protein quantification assay

The protein content of the EV fractions was quantified using Pierce BCA Protein Assay Kit (Thermo Scientific) according to the manufacturer's instructions (figure 10). EV were first lysed using 1x RIPA lysis buffer (Fisher Scientific). Incubation for lysis was done for 10 min at 4°C. Lysates were then diluted in PBS buffer (10 mM, pH 7.4) by 1:50. Samples were distributed on a 96-well microplate and mixed with the working solution, prepared as instructed in the manual. 9 dilutions were used as standards, using BSA and ranging from 0 to 2,000 μ g/ml. All samples and standards were done in duplicate. Solutions were incubated in the plate for 30 min at 37°C. Then, a photometric measurement at 562 nm was taken using a microplate reader (ThermoScientific, Varioskan Flash). A calibration curve was done with the standards, using a polynomial function of second or third order to fit the data. Conversion of output data into concentrations was done using the resulting formula with the better fit.

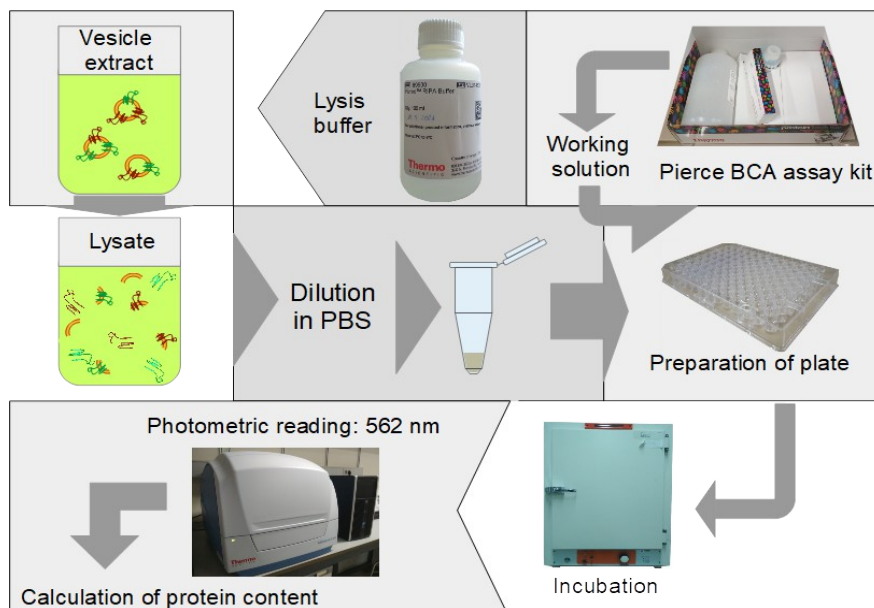


Figure 10: quantification of total protein content on EV extract using the Pierce BCA protein assay kit.

3.7. Size measurements by DLS

In order to monitor the conjugation of AuNPs with the antibodies, the nanoparticles were characterized by Dynamic Light Scattering (DLS) (MALVERN instruments, Zetasizer Nano, shown in figure 11). The hydrodynamic diameters of AuNPs with or without the antibody on their surface were compared. For this, conjugated and non conjugated AuNPs were diluted to 1:50 in water and their hydrodynamic diameters were measured using the AuNPs GEAB SOP (standard operating procedure). Figure 12 shows the size distribution of the AuNPs before and after conjugation, evidencing the increase in the hydrodynamic diameter caused by the presence of proteins in the surface of the conjugated nanoparticles.



Figure 11: Zetasizer Nano (MALVERN instruments). Samples were diluted and measured by DLS in order to determine the size of the analytes.

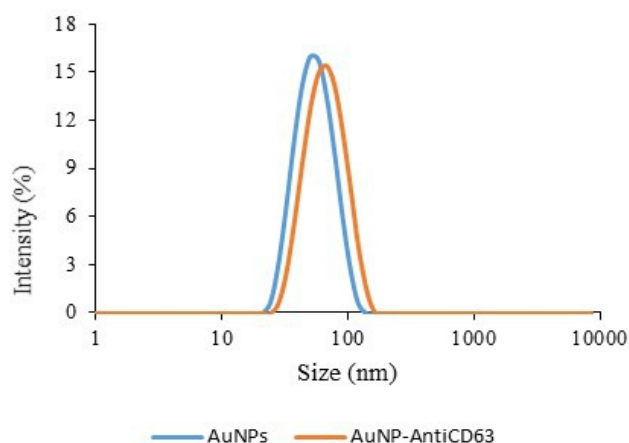


Figure 12: size distribution of gold nanoparticles before and after conjugation with anti-CD63 antibodies. In this case, the average hydrodynamic diameter of pure AuNPs was 57 nm, and 70 nm for conjugated AuNPs,.

The size distribution of EV fractions from CRC and control patients were also analyzed by DLS: the samples were diluted to 1:100 in HEPES (10 mM, pH 7.4) and analyzed using the SOP Exosomes GEAB.

3.8. Statistical analysis

3.8.1. Removal of outliers

Data deviating excessively from the distribution was removed prior to analysis. Cutoff distance was the 0.25 or the 0.75 quartile plus 1.5 times the interquartile distance. Data was not subjected to this procedure in case of a small number of samples in a group.

3.8.2. Data treatment

Data from different groups was compared in order to detect statistical differences. Parametric tests were used whenever possible, due to having higher sensitivity than equivalent non-parametric tests. Requirements for a parametric test were: sample number > 5 on each group, normal distribution of data within each group (verified using a Shapiro-Wilk test) and equality of variances of all compared groups (F-test when comparing two groups, Bartlett test for more than two groups). If a parametric analysis was not possible, a non parametric tests was used instead. Since group II presented less than five samples, parametric tests were performed when possible by excluding this group, followed by a non-parametric test with all groups.

Differences between two groups were analyzed with Student's T-test. For Comparisons between more than two groups, a one-way ANOVA was used as the parametric alternative, and a Kruskal-Wallis test was used as the non parametric test. Afterwards, groups were compared using the post hoc Tukey's Honest Significant Differences test for a parametric approach and Dunn's test (using the Bonferroni correction) for a non-parametric approach. Threshold for significant difference was set at 0.05. Data were analyzed using R version 4.1.3 (www.r-project.org).

4. Results

4.1. Characterization of extracellular vesicles

4.1.1. Size distribution

In a previous study (Pérez-Botas, 2020) the size distribution profiles and the concentration of freshly isolated EVs from each clinical group of patients were analyzed by nanoparticle tracking analysis (NTA). The results showed no statistical differences between the groups. Nevertheless, in the present study, EV fractions from a small cohort of patients were analyzed by a different technique, DLS. NTA presents analytical advantages to DLS: it is more suitable for polydisperse samples, and it can provide more information, such as particle concentration. However, it requires a specialized operator, expensive equipment and a more extensive preparation process. Samples from 10 patients of group I (control), 4 patients of group II and 10 patients of group IV were analyzed, and the main peak detected was used for comparisons. Figure 13 shows the size distribution profiles:

Overall, the sizes in the three groups of patients range between 75 and 150 nm. Therefore, these EV may be considered small EVs (sEVs), in accordance with the International Society of Extracellular Vesicles (Théry *et al.*, 2018).

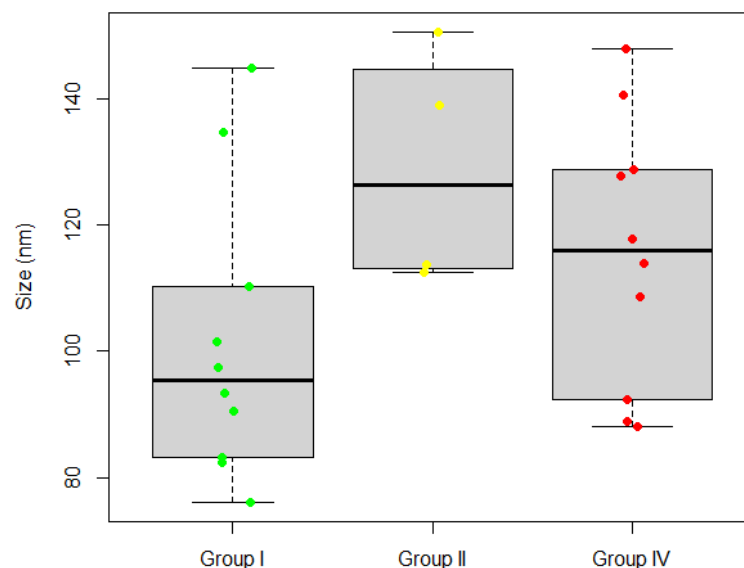


Figure 13: Size distribution of EVs based on their hydrodynamic diameter, measured by DLS.

Groups I, II and IV were statistically compared (Table 3) using a Kruskal-Wallis test followed by a Dunn's test. Smaller EV sizes were observed in group I compared with the other groups, although this trend did not reach statistical significance.

Table 3: Statistical comparison of clinical groups based on size distribution (hydrodynamic diameter based on DLS).

Kruskal-Wallis test	Dunn's test (Bonferroni correction)		Student's T-test		
p-value	p-value by groups	I	II	Alternative hypothesis	p-value
0.097	II	0.062	-	I and IV are different	0.17
	IV	0.232	0.5	I is lower than IV	0.085

A Student's T-test was used to compare groups I and IV. Statistical difference was not found, although analysis under the assumption that $I < IV$ was close to being statistically significant (p-value 0.085).

A statistical difference between groups cannot be concluded through this data. However, size differences between groups may indicate a greater EV diameter in CRC patients.

4.1.2. Total protein content

Total protein content was calculated through a BCA assay kit for all samples in the cohort (Figure 14). Table 4 summarizes the statistical analysis carried out to compare the total protein concentration between the groups.

Comparison between all groups (Kruskal-Wallis and Dunn's test) indicated a p-value (0.059) close to the significance threshold. The protein concentration in group IV was significantly higher in comparison with group III ($p = 0.049$, Dunn's test).

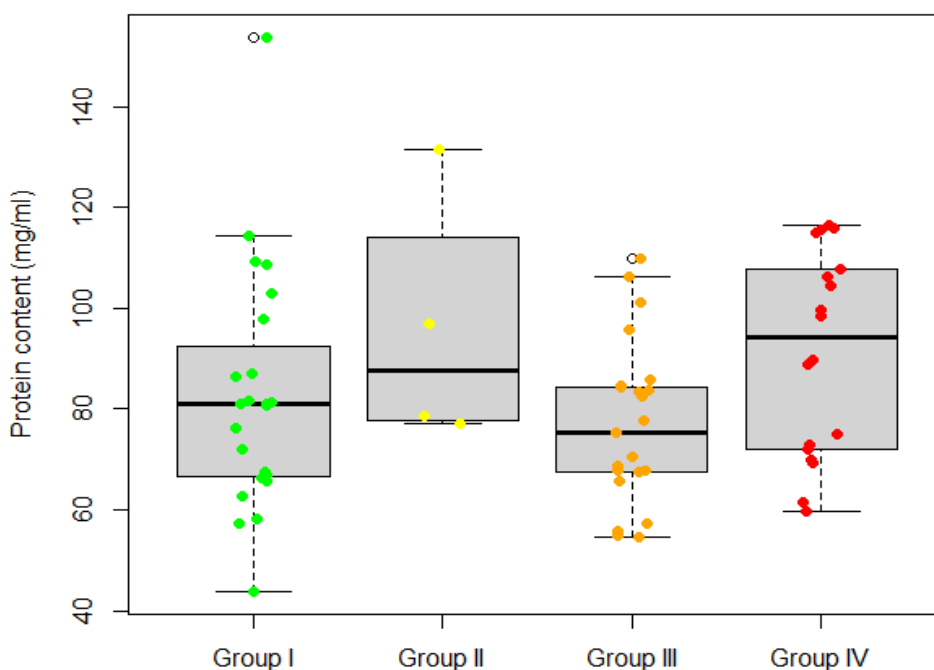


Figure 14: Protein content of samples by group, calculated using a BCA assay.

Table 4: Statistical comparison of protein content, measured using a BCA assay kit, in clinical groups.

Kruskal-Wallis test	Dunn's test (Bonferroni correction)	ANOVA			Tukey's test			
p-value	p-value by groups	I	II	III	p-value	p-value by groups	I	III
0.059	II	0.601	-	-	0.024	III	0.739	-
	III	1	0.311	-		IV	0.112	0.022
	IV	0.212	1	0.049				

This result was verified by a one-way ANOVA. A significant difference was found ($p = 0.024$), and the post-hoc test confirmed the difference between groups III and IV ($p = 0.022$). Further analysis could be of use to verify this finding, in order to determine whether this difference is due to a modification of EVs or to the presence of free proteins co-precipitated during EV purification.

Since various proteins are expressed in EVs, a relationship between size and protein content could be expected. Nevertheless, this relationship was not found (Figure 15). However, since EV sizes for group III were not measured, it is not possible to study this relationship between groups III and IV, which presented significant difference in protein content.

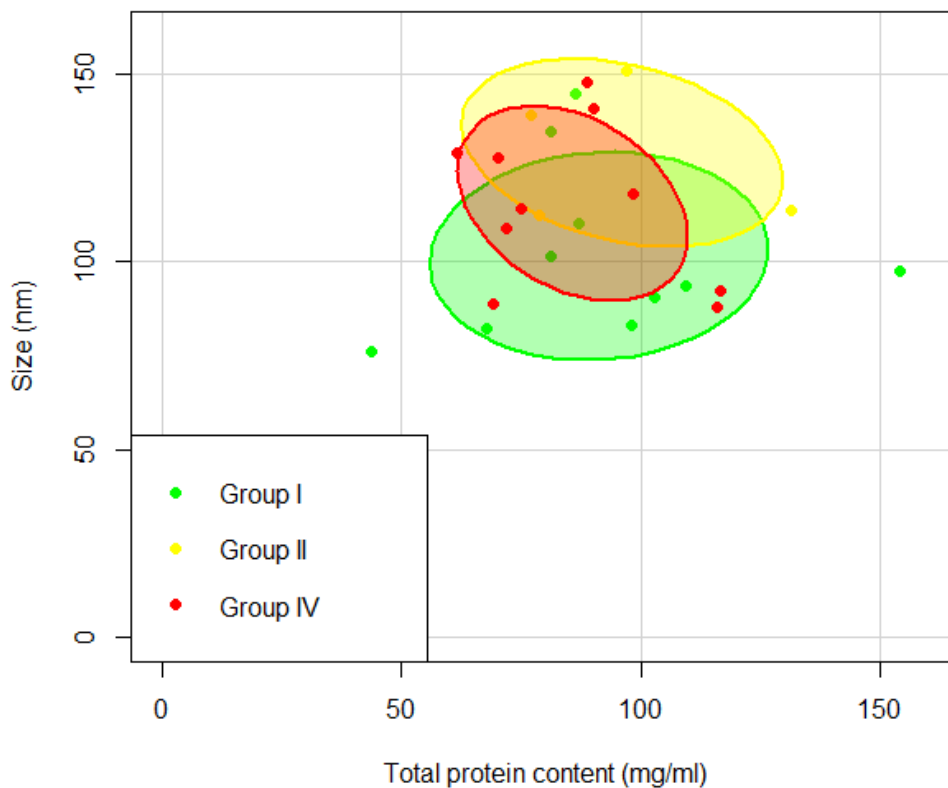


Figure 15: Representation of total protein content by EV size, coloured differently based on the clinical groups.

4.2. Analysis of surface EV biomarkers

4.2.1. Analysis of CD9⁺ EV by lateral flow immunoassay

Tetraspanins such as CD9, CD63 and CD81 are present in most EVs, with higher levels of expression than in cells (Doyle and Wang, 2019, Hon *et al.*, 2017). In the present study, an antibody targeting CD63 was used to bind EVs to AuNPs used for detection. A different marker was used to immobilize the resulting complex on the antibody test lines, with the line intensity after binding as the abundance of EVs containing said marker (Figure 16). For the purpose of this study, CD9 intensity was interpreted as total EV content in samples.

Differences between clinical groups were verified (Table 5), and significance was found ($p = 0.00045$, ANOVA). Significant differences were found between groups I and IV ($p = 0.00028$), and groups III and IV ($p = 0.031$, Tukey's test), where group IV presented the lowest intensity

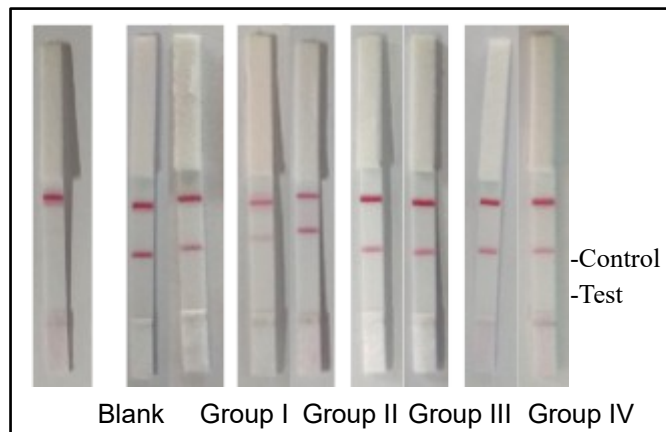


Figure 16: LFIAs from multiple patients for the detection of CD9⁺-EVs.

(Figure 17). No statistical differences were found between group II and the others (Dunn's test).

With CD9 intensity being used as an estimate of EV abundance, greater signal intensities could involve higher protein content or greater sizes. Therefore, a relationship between CD9 intensities and protein concentration or vesicle size was analyzed. However, The differences found in signal intensities did not correlate with the results on protein concentration or size previously obtained. (Figure 18).

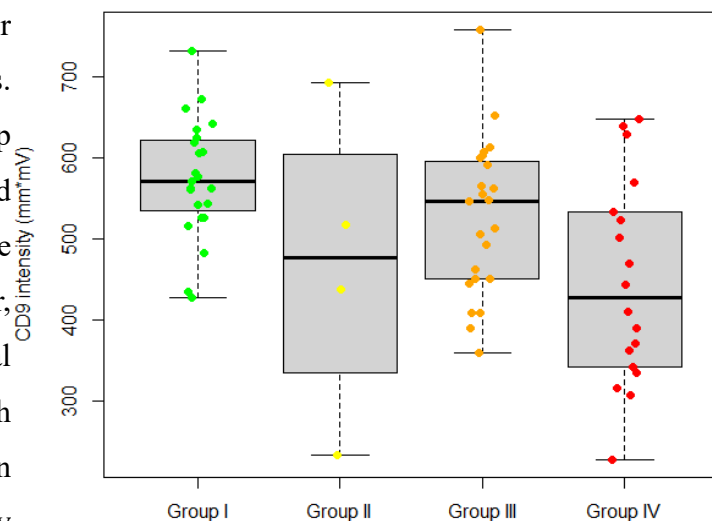


Figure 17: Intensity of CD9 marker by group. Significant difference was found between groups I and IV, and between III and IV.

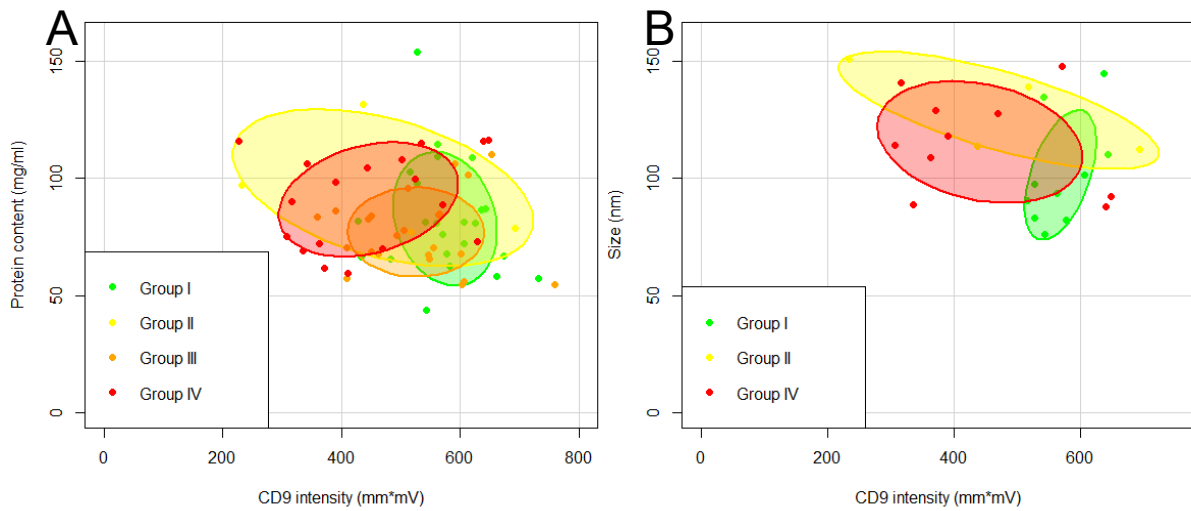


Figure 18: Scatterplots showing the relation between CD9 intensity and protein concentration (A) and EV size (B).

Table 5: Statistical comparison of CD9 intensity (Representing total EV number) in clinical groups.

Kruskal-Wallis test	Dunn's test (Bonferroni correction)			ANOVA	Tukey's test			
p-value	p-value by groups	I	II	III	p-value	p-value by groups	I	III
0.0079	II	0.441	-	-	0.00045	III	0.219	-
	III	0.287	1	-		IV	0.00028	0.031
	IV	0.0021	1	0.203				

4.2.2. CD147 and EpCAM markers in CRC diagnosis

Overexpression of proteins CD147 and EpCAM has been previously linked to cancer, and in particular, to CRC (Liu H. *et al.*, 2021, Yoshioka *et al.*, 2014, Tauro *et al.*, 2013). Therefore, assessment of the relationship between CD147⁺ and EpCAM⁺-EVs and the clinical groups of the cohort was performed in order to evaluate their potential as CRC biomarkers. CD147 and EpCAM intensities on the test line was considered as the total count of CD147⁺ and EpCAM⁺-EVs respectively (Figure 19). In order to normalize values among patients, ratios CD147/CD9 and EpCAM/CD9 were calculated and tested. These parameters can be considered an estimation of the proportion of CD147⁺ and EpCAM⁺-EVs in relation of the total number of EV (CD9⁺-EV).

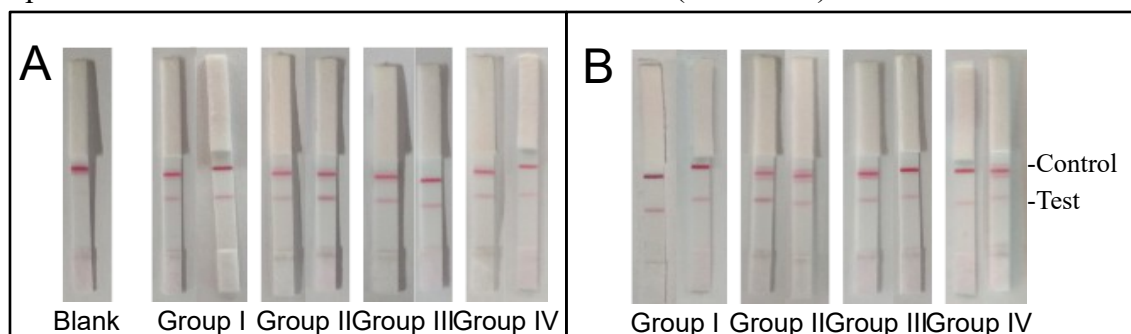


Figure 19: LFIAs from multiple patients for the detection of CD147⁺-EVs (A) and EpCAM⁺-EVs (B).

Statistical comparisons of CD147 intensities are shown in Table 6. Statistical difference between groups I, III and IV was found ($p = 0.0063$, ANOVA). Signal intensity corresponding to CD147⁺-EV was significantly lower in the CRC group than in groups I and III (Figure 20 (A)) No additional differences were found with group II.

Regarding the analysis of EpCAM⁺-EV, the assumptions for ANOVA were not met. Therefore, only the Kruskal-Wallis test and Dunn's test were performed (Table 7). No significant difference was found (p-value of 0.157), although, EpCAM may follow the same trend observed in CD9 and CD147, presenting lower intensities in group IV (Figure 20 (B)).

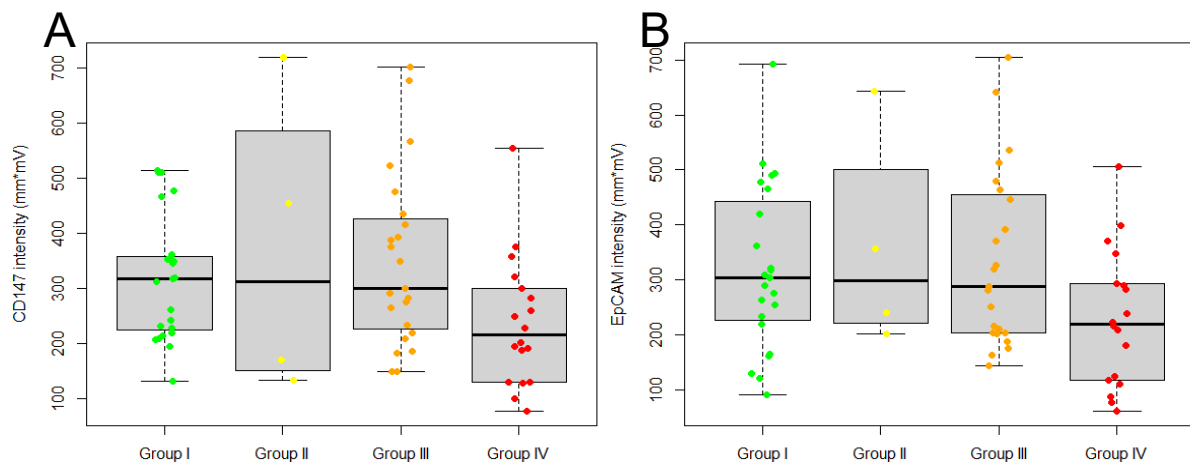


Figure 20: Signal intensities measured in the test line corresponding to CD147⁺-EV (A) and EpCAM⁺-EV (B) on each clinical group. In both cases, a decreasing trend was observed, with group IV presenting the lowest intensities.

Table 6: Statistical comparison of CD147 intensity (Representing CD147⁺-EVs) in clinical groups.

Kruskal-Wallis test p-value	Dunn's test (Bonferroni correction)			ANOVA p-value	Tukey's test		
	p-value by groups	I	II		III	I	III
0.07	II	1	-	0.0063	III	0.688	-
	III	1	1		IV	0.042	0.0055
	IV	0,1	0,931		0.04		

Table 7: Statistical comparison of EpCAM intensity (Representing EpCAM⁺-EVs) in clinical groups.

Kruskal-Wallis test p-value	Dunn's test (Bonferroni correction)			
	p-value by groups	I	II	III
0.157	II	1	-	-
	III	1	1	-
	IV	0,166	0.569	0.137

Despite the differences found on single detection of CD147⁺ and EpCAM⁺-EV, no statistical differences between groups were found when comparing the ratios CD147/CD9 and EpCAM/CD9 (Figure 21, Figure 22). Introduction of group II through non-parametric tests confirmed the absence of statistical differences (Table 8 and Table 9 respectively). Since CD9, CD147 and EpCAM intensities all presented a similar trend, with lower values in more advanced groups, the absence of significant differences in the ratios is logical. However, it is yet to be explained why this trend is shared by all markers, and if it is due to the alteration of EV populations or to another factor.

As for CD147/EpCAM ratio, indicating the relative abundance of EVs expressing the mentioned markers, no observable differences between groups were present (Figure 23), and average ratio was close to 1, which may indicate a very similar occurrence of both markers in EVs.

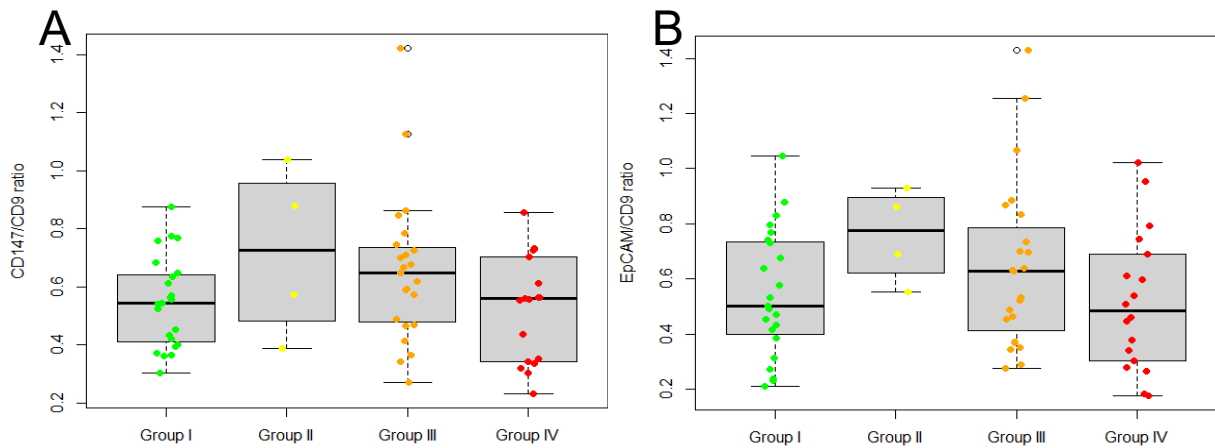


Figure 21: CD147/CD9 intensity ratio by clinical group (A). EpCAM/CD9 intensity ratio by clinical group (B).

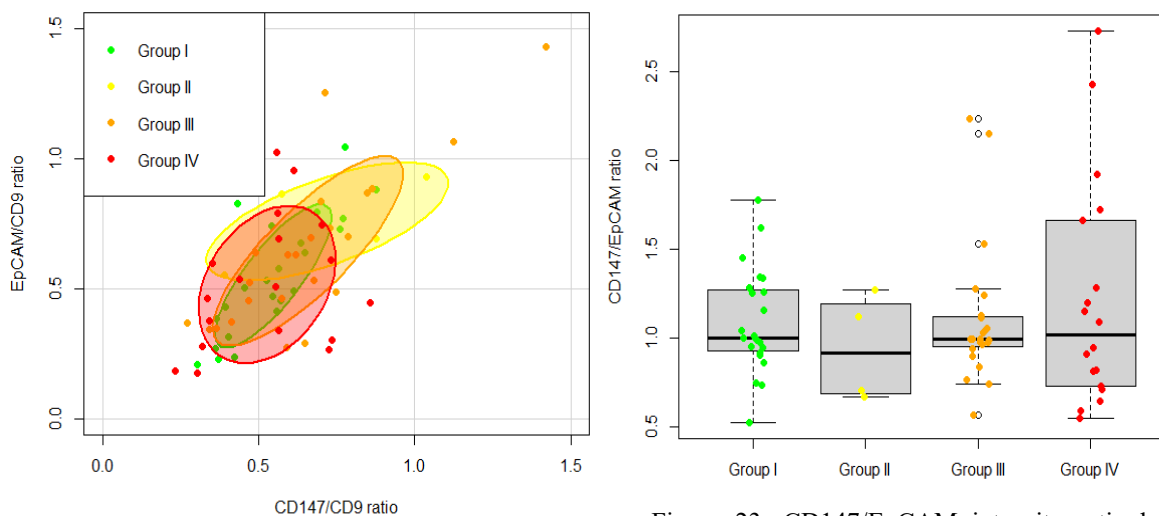


Figure 22: Representation of the relationship between intensity ratios CD147/CD9 and EpCAM/CD9. Note that group II is slightly offset from the other groups.

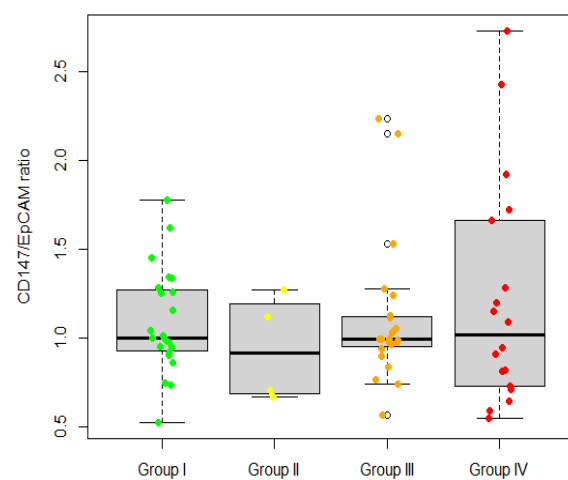


Figure 23: CD147/EpCAM intensity ratio by clinical group. Since ratios are close to 1, occurrence of CD147⁺ and EpCAM⁺-EVs is likely similar.

Table 8: Statistical comparison of CD147/CD9 intensity ratio (Representing the CD147⁺-EV fraction of the total EVs) in clinical groups.

Kruskal-Wallis test	Dunn's test (Bonferroni correction)			ANOVA	Tukey's test			
p-value	p-value by groups	I	II	III	p-value	p-value by groups	I	III
0.271	II	0.509	-	-	0.383	III	0.565	-
	III	0.797	1	-		IV	0.925	0.38
	IV	1	0.352	0.464				

Table 9: Statistical comparison of EpCAM/CD9 intensity ratio (Representing the EpCAM⁺-EV fraction of the total EVs) in clinical groups.

Kruskal-Wallis test	Dunn's test (Bonferroni correction)			ANOVA	Tukey's test			
p-value	p-value by groups	I	II	III	p-value	p-value by groups	I	III
0.234	II	0.277	-	-	0.478	III	0.692	-
	III	1	0.574	-		IV	0.906	0.465
	IV	1	0.158	0.771				

4.3. Pilot study: effect of freezing-thawing EV fractions

The isolated EV fractions were stored at -80°C upon LFIA analysis. In order to prevent a bias in LFIA induced by the freezing and thawing of the sample, tests were performed with fresh, recently isolated EV extracts. Although the isolation method employed in this study enables the handling of several clinical samples simultaneously, the processing rate of samples could be enhanced if isolation and testing were done separately, with a greater number of samples. To achieve this goal, a stable conservation of EVs is required.

In order to verify the repeatability of the results in frozen samples, a total number of 16 samples were re-tested for the CD9 marker after one month at -80°C. Results showed no clear correlation between the first and second measure, but the latter presented a statistically lower mean value (Figure 24) than the one in fresh samples (p-value 0.032, paired Student's T-test).

Due to the high variability of the results, it is not possible to accurately predict the modification of the signal intensity in frozen samples. Therefore, for further standardization and simplification of our LFIA procedure, seeking an adequate preservative agent would be required.

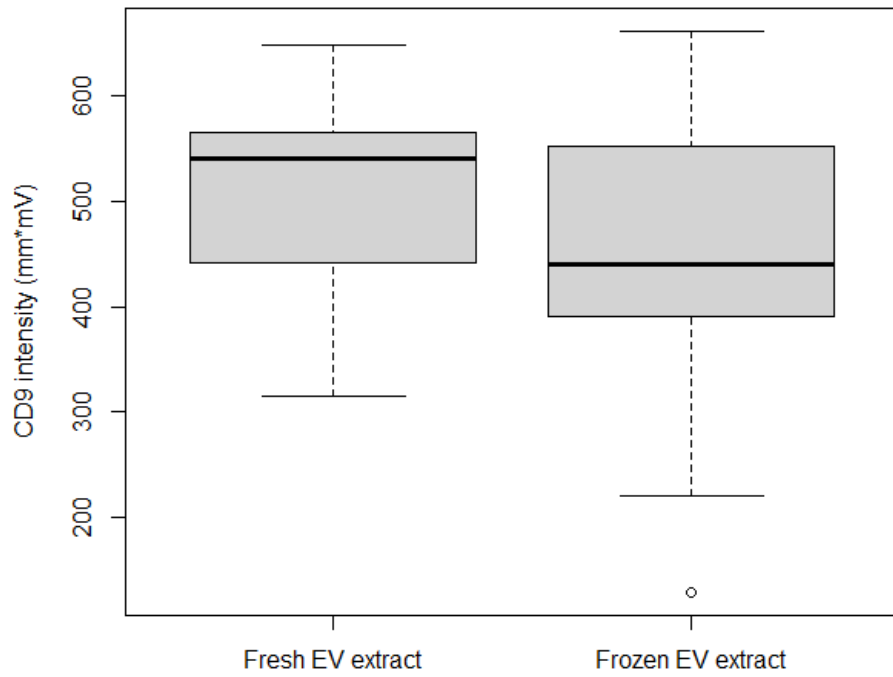


Figure 24: CD9 intensity for fresh EVs and for frozen EVs, kept at -80°C for one month.

5. Discussion

This work aimed to study surface markers in circulating extracellular vesicles in patients at different stages of colorectal cancer. To this end, plasma-derived EV were isolated, characterized, and subsequently analyzed by LFIA in order to identify potential CRC biomarkers.

The CRC group presented higher average EV size values than the control group, although no significant differences were found, in correspondence to previous observations from our research team (Pérez-Botas, 2020). A statistical difference was found in the protein content of EVs from patients with CRC, which was found higher than in the other groups. Total protein content accounts not just for the EV-associated proteins, since the isolation method by a precipitation reagent presents low specificity and it co-isolates contaminants. Therefore, further characterization would be required in order to determine whether this difference is linked to the EVs themselves or to the presence of non-EV protein components.

CD9 belongs to the tetraspanin superfamily, a group of transmembrane proteins expressed in a wide variety of cells. Tetraspanins have four transmembrane domains, and act as organizers of the membrane through interactions with other proteins. They are involved in many processes, such as cell adhesion, motility, signal transduction, cell differentiation, etc (Brosseau *et al.*, 2018). CD9 accomplishes a number of functions, such as the regulation of a variety of cell types, stem cell differentiation, and inflammation. Its involvement in cancer is controversial. While in some cases its expression is correlated with a higher survival chance and its downregulation is associated with bad outcome in a variety of cancers, other works showed that in other cases, such as acute lymphoblastic leukemia, CD9 expression relates to poor prognostics (Brosseau *et al.*, 2018). In the present research, CD9 intensity measured in the LFIA could not be associated with neither protein content nor EV size. However, since the total protein content includes contaminants, the possibility of a link between CD9⁺-EV content and protein content can not be ruled out until a new analysis using a more specific purification method is done. For CD9 intensity, a significant difference was found, indicating lower values for the CRC group than for the control and high-grade adenoma. This may indicate a decrease in CD9⁺-EVs, in contrast to the increase in protein content. Since CD9 expression is known to decrease in some cancer, in

particular at later stages, this result does not contradict existing knowledge.

CD147 is a transmembrane glycoprotein of the immunoglobulin superfamily involved in a variety of functions such as cell adhesion, migration, differentiation, secretion and inflammatory response (Muramatsu and Miyauchi, 2003). It has been associated with important roles in reproduction and nervous function, and it is also known to be essential for the process of HIV-1 infection. Moreover, this protein is found overexpressed in tumor cell, and can induce matrix metalloproteases production and release, which promote tumor invasion (Yoshioka *et al.*, 2014, Muramatsu and Miyauchi, 2003). EpCAM, or CD326, is a type I transmembrane glycoprotein and presents a variety of functions in epithelial tissues: cell-to-cell junctions, cellular motility, cell proliferation and signaling. It is an important protein during embryo development, and also presents functions in adults (Huang *et al.*, 2018). This molecule is often overexpressed in tumors, and it is involved in tumor invasion and metastasis (Liu H. *et al.*, 2021, Tauro *et al.*, 2013, Huang *et al.*, 2018). Patients with CRC showed the lowest intensities when analyzing CD147⁺-EV by LFIA, and this difference was statistically significant. Regarding EpCAM, a similar trend was found, although differences were not significant. This could be due to data noise as well as decreased accuracy of the statistical test (data did not follow a normal distribution, therefore ANOVA was not used for the statistical analysis). While the decrease in CD9 intensity in CRC samples is in line with existing information, decrease of CD147 and EpCAM is not. Existing research indicates an increase in expression rate in CRC patients for both proteins, often associated with bad prognostics for cancer (Liu H. *et al.*, 2021, Yoshioka *et al.*, 2014, Tauro *et al.*, 2013, Muramatsu and Miyauchi, 2003, Huang *et al.*, 2018). Our result may be explainable when considering tetraspanin CD63. While not directly measured, our LFIA can only detect CD63⁺-EVs, and a decrease on this population could affect all our results simultaneously. CD63 is a known tumor repressor, enhancing cell adhesion and preventing metastasis, and in lung and ovarian cancer tumor progression has been associated to decreased CD63 expression (Titu *et al.*, 2021). On the other hand, a histological study revealed that CD63 levels were directly correlated to poor prognosis in CRC (Tuomas *et al.*, 2020).

CD147/CD9 and EpCAM/CD9 ratios were calculated in order to normalize results. Whereas CRC patients showed lower intensities when measuring CD9⁺, CD147⁺ and EpCAM⁺-EVs, no significant differences in the ratios were found among any of the groups.

Due to the low specificity of the precipitation methods for EV isolation, proteins and other elements co-precipitate with the EVs. However, the choice of the purification method was done due to its simplicity and short processing time, properties necessary for a PoC biosensor intended for extensive screening. The use of a more complex method could render the analysis more cumbersome. Therefore a balance between simplicity and extract quality (purity and yield) should be achieved, by either changing the purification technique or adding in new steps to the current one (*e.g.* ultrafiltration, SEC). Additionally, immuno-magnetic separation procedures could be used to remove EV populations that are of no interest for our analysis. By removing contaminants as well as EVs of no interest, the sample would be enriched in the EV population of interest and might offer more significant results.

Since all markers followed the same trend, instead of a difference in the levels of CD9⁺, CD147⁺ and EpCAM⁺-EVs, the presented results might indicate an external factor influencing all results, and since this factor operates differently in CRC patients, it could become a marker on itself. CD63, as previously mentioned, could be this factor, but the current results are not enough to verify this hypothesis. By using different combinations of detection antibodies (bound to AuNPs) and capture antibodies (bound to test lines) a more comprehensive knowledge of the changes in the various EV populations in patients of different clinical groups could be acquired, enabling an optimal choice of markers.

Finally, results from the pilot study assessing the effect of freezing-thawing EV fractions revealed that current storing processes pose an issue for EV stability. The use of a preservative agent on isolated EV fractions will be a necessary step for further standardization of our LFIA.

6. Conclusions

- We have successfully created a working AuNP-based LFIA capable of analyzing small volumes of purified EV samples for semiquantitative analysis.
- We have verified that markers CD9, CD147 and EpCAM showed lower intensity values in our LFIA for CRC patients, contrary to their expected increase. However, those differences might not be due to a modification of EV populations containing the mentioned markers. Instead, a fluctuation in CD63⁺-EVs could be responsible for those results. Further research is required into this subject.
- The EV purification technique using a precipitation reagent presented low specificity. Improvements in this procedure are necessary for an optimal measurement.
- Insights in the process of freezing-thawing used for EV conservation revealed that EV stability is not guaranteed and that LFIA signal may be affected when using frozen samples. Inclusion of a conservative agent is necessary for standardization of our LFIA.

7. Bibliography

Brosseau, C., Colas, L., Magnan, A., & Brouard, S. (2018). CD9 tetraspanin: A new pathway for the regulation of inflammation? In *Frontiers in Immunology* (Vol. 9, Issue OCT). Frontiers Media S.A.

Castro-Marrero, J., Serrano-Pertierra, E., Oliveira-Rodríguez, M., Zaragozá, M. C., Martínez-Martínez, A., Blanco-López, M. del C., & Alegre, J. (2018). Circulating extracellular vesicles as potential biomarkers in chronic fatigue syndrome/myalgic encephalomyelitis: an exploratory pilot study. *Journal of Extracellular Vesicles*, 7(1).

Chen, J., Li, P., Zhang, T., Xu, Z., Huang, X., Wang, R., & Du, L. (2022). Review on Strategies and Technologies for Exosome Isolation and Purification. In *Frontiers in Bioengineering and Biotechnology* (Vol. 9). Frontiers Media S.A.

Chen, Y., Xie, Y., Xu, L., Zhan, S., Xiao, Y., Gao, Y., Wu, B., & Ge, W. (2017). Protein content and functional characteristics of serum-purified exosomes from patients with colorectal cancer revealed by quantitative proteomics. *International Journal of Cancer*, 140(4), 900–913.

Chettimada, S., Lorenz, D. R., Misra, V., Dillon, S. T., Reeves, R. K., Manickam, C., Morgello, S., Kirk, G. D., Mehta, S. H., & Gabuzda, D. (2018). Exosome markers associated with immune activation and oxidative stress in HIV patients on antiretroviral therapy. *Scientific Reports*, 8(1).

Dai, J., Su, Y., Zhong, S., Cong, L., Liu, B., Yang, J., Tao, Y., He, Z., Chen, C., & Jiang, Y. (2020). Exosomes: key players in cancer and potential therapeutic strategy. In *Signal Transduction and Targeted Therapy* (Vol. 5, Issue 1). Springer Nature.

Doyle, L. M., & Wang, M. Z. (2019). Overview of extracellular vesicles, their origin, composition, purpose, and methods for exosome isolation and analysis. In *Cells* (Vol. 8, Issue 7). MDPI.

Feng, K., Ma, R., Zhang, L., Li, H., Tang, Y., Du, G., Niu, D., & Yin, D. (2020). The Role of Exosomes in Thyroid Cancer and Their Potential Clinical Application. In *Frontiers in Oncology* (Vol. 10). Frontiers Media S.A.

Gurung, S., Perocheau, D., Touramanidou, L., & Baruteau, J. (2021). The exosome journey: from biogenesis to uptake and intracellular signalling. In *Cell Communication and Signaling* (Vol. 19, Issue 1). BioMed Central Ltd.

Han, Y. M., & Im, J. P. (2016). Colon capsule endoscopy: Where are we and where are we going. In *Clinical Endoscopy* (Vol. 49, Issue 5, pp. 449–453). Korean Society of Gastrointestinal Endoscopy.

Hon, K. W., Abu, N., Ab Mutalib, N. S., & Jamal, R. (2017). Exosomes as potential biomarkers and targeted therapy in colorectal cancer: A mini-review. In *Frontiers in Pharmacology* (Vol. 8, Issue AUG, p. 583). Frontiers Media S.A.

- Huang, L., Yang, Y., Yang, F., Liu, S., Zhu, Z., Lei, Z., & Guo, J. (2018). Functions of EpCAM in physiological processes and diseases (Review). In *International Journal of Molecular Medicine* (Vol. 42, Issue 4, pp. 1771–1785). Spandidos Publications.
- Kim, K. Y., Shin, K. Y., & Chang, K. A. (2021). Brain-derived exosomal proteins as effective biomarkers for alzheimer's disease: A systematic review and meta-analysis. In *Biomolecules* (Vol. 11, Issue 7). MDPI.
- Kowal, J., Tkach, M., & Théry, C. (2014). Biogenesis and secretion of exosomes. In *Current Opinion in Cell Biology* (Vol. 29, Issue 1, pp. 116–125). Elsevier Ltd.
- Liu, H., Qiao, S., Fan, X., Gu, Y., Zhang, Y., & Huang, S. (2021). Role of exosomes in pancreatic cancer (Review). In *Oncology Letters* (Vol. 21, Issue 4). Spandidos Publications.
- Liu, Y., Zhan, L., Qin, Z., Sackrison, J., & Bischof, J. C. (2021). Ultrasensitive and Highly Specific Lateral Flow Assays for Point-of-Care Diagnosis. In *ACS Nano* (Vol. 15, Issue 3, pp. 3593–3611). American Chemical Society.
- Logozzi, M., Mizzoni, D., di Raimo, R., & Fais, S. (2020). Exosomes: A source for new and old biomarkers in cancer. In *Cancers* (Vol. 12, Issue 9, pp. 1–18). MDPI AG.
- Matsumura, T., Sugimachi, K., Iinuma, H., Takahashi, Y., Kurashige, J., Sawada, G., Ueda, M., Uchi, R., Ueo, H., Takano, Y., Shinden, Y., Eguchi, H., Yamamoto, H., Doki, Y., Mori, M., Ochiya, T., & Mimori, K. (2015). Exosomal microRNA in serum is a novel biomarker of recurrence in human colorectal cancer. *British Journal of Cancer*, *113*(2), 275–281.
- Muralidharan-Chari, V., Clancy, J. W., Sedgwick, A., & D'Souza-Schorey, C. (2010). Microvesicles: Mediators of extracellular communication during cancer progression. In *Journal of Cell Science* (Vol. 123, Issue 10, pp. 1603–1611).
- Muramatsu, T., & Miyauchi, T. (2003). Basigin (CD147) a multifunctional transmembrane protein involved in reproduction, neural function, inflammation and tumor invasion. *Histol Histopathol*, *18*(3), 981–987.
- Núñez, O., Rodríguez Barranco, M., Fernández-Navarro, P., Redondo Sanchez, D., Luque Fernández, M. Á., Pollán Santamaría, M., & Sánchez, M. J. (2020). Deprivation gap in colorectal cancer survival attributable to stage at diagnosis: A population-based study in Spain. *Cancer Epidemiology*, *68*.
- Pérez-Botas, H. (2020). Characterization of circulating extracellular vesicles and detection of the CD147 biomarker in a cohort of patients with colorectal cancer at the Hospital Universitario de San Agustín. Master's thesis at the University of Oviedo.
- Qu, A., Du, L., Yang, Y., Liu, H., Li, J., Wang, L., Liu, Y., Dong, Z., Zhang, X., Jiang, X., Wang, H., Li, Z., Zheng, G., & Wang, C. (2014). Hypoxia-inducible MiR-210 is an independent prognostic factor and contributes to metastasis in colorectal cancer. *PLoS ONE*, *9*(3).

Reclusa, P., Taverna, S., Pucci, M., Durendez, E., Calabuig, S., Manca, P., Serrano, M. J., Sober, L., Pauwels, P., Russo, A., & Rolfo, C. (2017). Exosomes as diagnostic and predictive biomarkers in lung cancer. In *Journal of Thoracic Disease* (Vol. 9, pp. S1373–S1382). AME Publishing Company.

Sawicki, T., Ruszkowska, M., Danielewicz, A., Niedźwiedzka, E., Arłukowicz, T., & Przybyłowicz, K. E. (2021). A review of colorectal cancer in terms of epidemiology, risk factors, development, symptoms and diagnosis. In *Cancers* (Vol. 13, Issue 9). MDPI AG.

Serrano-Pertierra, E., Oliveira-Rodríguez, M., Matos, M., Gutiérrez, G., Moyano, A., Salvador, M., Rivas, M., & Blanco-López, M. C. (2020). Extracellular vesicles: Current analytical techniques for detection and quantification. In *Biomolecules* (Vol. 10, Issue 6). MDPI AG.

Shen, M., Di, K., He, H., Xia, Y., Xie, H., Huang, R., Liu, C., Yang, M., Zheng, S., He, N., & Li, Z. (2020). Progress in exosome associated tumor markers and their detection methods. *Molecular Biomedicine*, 1(1).

Skotland, T., Ekroos, K., Kauhanen, D., Simolin, H., Seierstad, T., Berge, V., Sandvig, K., & Llorente, A. (2017). Molecular lipid species in urinary exosomes as potential prostate cancer biomarkers. *European Journal of Cancer*, 70, 122–132.

St John, A., & Price, C. P. (2014). Existing and Emerging Technologies for Point-of-Care Testing. *Clin Biochem Rev*, 35(3), 155–167

Strul, H., & Arber, N. (2002). Fecal occult blood test for colorectal cancer screening. *Annals of Oncology*, 13(1), 51–56.

Tauro, B. J., Greening, D. W., Mathias, R. A., Mathivanan, S., Ji, H., & Simpson, R. J. (2013). Two distinct populations of exosomes are released from LIM1863 colon carcinoma cell-derived organoids. *Molecular and Cellular Proteomics*, 12(3), 587–598.

Théry, C., Witwer, K. W., Aikawa, E., Jose Alcaraz, M., Anderson, J. D., Andriantsitohaina, R., Antoniou, A., Bach, M., Bachurski, D., Baharvand, H., Balaj, L., Baldacchino, S., Bauer, N. N., Baxter, A. A., Bebawy, M., Beckham, C., Bedina Zavec, A., Benmoussa, A., Berardi, A. C., ... Jung, S. (2018). Minimal information for studies of extracellular vesicles 2018 (MISEV2018): a position statement of the International Society for Extracellular Vesicles and update of the MISEV2014 guidelines. *Journal of Extracellular Vesicles*, 7(1).

Titu, S., Grapa, C. M., Mocan, T., Balacescu, O., & Irimie, A. (2021). Tetraspanins: Physiology, colorectal cancer development, and nanomediated applications. In *Cancers* (Vol. 13, Issue 22). MDPI.

Tricarico, C., Clancy, J., & D'Souza-Schorey, C. (2017). Biology and biogenesis of shed microvesicles. In *Small GTPases* (Vol. 8, Issue 4, pp. 220–232). Taylor and Francis Inc.

Tuomas Kaprio, Jaana Hagström, Leif C Andersson, & Caj Haglund. (2020). Tetraspanin CD63 independently predicts poor prognosis in colorectal cancer. *Histol*

Histopathol, 35(8), 887–892.

Van Niel, G., D'angelo, G., & Raposo, G. (2018). Shedding light on the cell biology of extracellular vesicles. *Nature Reviews Molecular Cell Biology*, 19(4), 213–228.

Yoshioka, Y., Kosaka, N., Konishi, Y., Ohta, H., Okamoto, H., Sonoda, H., Nonaka, R., Yamamoto, H., Ishii, H., Mori, M., Furuta, K., Nakajima, T., Hayashi, H., Sugisaki, H., Higashimoto, H., Kato, T., Takeshita, F., & Ochiya, T. (2014). Ultra-sensitive liquid biopsy of circulating extracellular vesicles using ExoScreen. *Nature Communications*, 5, 3591.

Zhang, Y., Liu, Y., Liu, H., & Tang, W. H. (2019). Exosomes: Biogenesis, biologic function and clinical potential. In *Cell and Bioscience* (Vol. 9, Issue 1). BioMed Central.

Zhang, Y., Xiao, Y., Sun, G., Jin, X., Guo, L., Li, T., & Yin, H. (2021). Harnessing the therapeutic potential of extracellular vesicles for cancer treatment. *Seminars in Cancer Biology*, 74, 92–104.

Zheng, G., Du, L., Yang, X., Zhang, X., Wang, L., Yang, Y., Li, J., & Wang, C. (2014). Serum microRNA panel as biomarkers for early diagnosis of colorectal adenocarcinoma. *British Journal of Cancer*, 111(10), 1985–1992.